

DIFFERENTIAL REQUIREMENTS FOR NONHOMOLOGOUS END-JOINING
(NHEJ) PATHWAY GENES IN DNA REPAIR

by

Nestor D. Rodriguez, B.S.

A thesis submitted to the Graduate Council of
Texas State University in partial fulfillment
of the requirements for the Degree of
Master of Science
with a Major in Biochemistry
May 2018

Committee Members:

L. Kevin Lewis, Chair

Karen A. Lewis

Wendi David

COPYRIGHT

by

Nestor D. Rodriguez

2018

FAIR USE AND AUTHOR'S PERMISSION STATEMENT

Fair Use

This work is protected by the Copyright Laws of the United States (Public Law 94-553, section 107). Consistent with fair use as defined in the Copyright Laws, brief quotations from this material are allowed with proper acknowledgment. Use of this material for financial gain without the author's express written permission is not allowed.

Duplication Permission

As the copyright holder of this work I, Nestor D. Rodriguez, authorize duplication of this work, in whole or in part, for educational or scholarly purposes only.

ACKNOWLEDGEMENTS

I would like to thank everyone in the Lewis lab who has helped contribute to this research project including Monica Wies, Shubha Malla, Angelica Riojas, Corbin England, Sarah Valencia, Alex Oviedo, and Racheal Russek as well as my two friends Kimer Long and Geraldo Medrano. The research done could not have been completed without your help. I would also like to thank my committee, Dr. Karen Lewis and Dr. Wendi David for the advice and comments given throughout this project. I would also like to thank my parents Gabriel and Juanita Rodriguez and the rest of my family for the emotional support and love throughout my educational career as well as my entire life. I would like to thank my research advisor as well as mentor throughout my undergraduate and graduate career, Dr. Kevin Lewis. He has taught me how to peruse research headstrong as well as helped mold me into a diligent scientist who questions rather than accepts. I will always look up to you as one of the most intelligent and wisest man I know and am glad I've had the opportunity to work for you for the past 4 years of my life, Thank you. Finally, I would like to thank all the Lewis labs from fall 2014 to spring 2018. This has by far been the most difficult journey of my life and a lot of hard work has been put into this thesis, but I am grateful for every moment.

TABLE OF CONTENTS

	Page
ACKNOWLEDGEMENTS	iv
LIST OF TABLES	vi
LIST OF FIGURES	vii
CHAPTER	
I. INTRODUCTION	1
II. MATERIALS AND METHODS	13
III. RESULTS AND DISCUSSION	22
IV. SUMMARY AND CONCLUSIONS	53
REFERENCES	58

LIST OF TABLES

Table	Page
1. Previous studies on NHEJ repair efficiency	9
2. Five other studies involving NHEJ repair assays on mid-log phase cells	57

LIST OF FIGURES

Figure	Page
1. Diagram of NHEJ pathway.....	4
2. The different levels of G ₁ phase cell cultures.....	5
3. Lack of homology within yeast cell.....	8
4. Traditional and modified transformation methods.....	10
5. Diagram of the plasmid pRS315URA3.....	23
6. Agarose gel electrophoresis (0.8%) of NcoI-cut and uncut pRS315URA3.....	24
7. Accurate and inaccurate repair of plasmids.....	25
8. Differences in NHEJ efficiencies of early stationary phase <i>S. cerevisiae</i> cells.....	27
9. NHEJ efficiencies of early stationary phase cells lacking subunits of the DNA ligase IV complex.....	29
10. NHEJ repair efficiencies of early stationary phase cells with mutations in Yku complex genes.....	31
11. NHEJ efficiencies of early stationary phase mutants lacking components of the Mrx complex.....	33
12. NHEJ efficiency tests of early stationary phase cells containing inactivated Mrx complex genes.....	34
13. Overhangs produced by digestion of plasmids with the three restriction enzymes used in this study.....	35
14. Agarose gel electrophoresis of NcoI-cut and AflIII-cut pRS315URA3.....	37
15. NHEJ efficiencies of early stationary phase cells using a 5' overhang-containing DSB in AflIII-cut pRS315URA3.....	38
16. pLKL67Y and pRS315 plasmids.....	39

17. NHEJ efficiencies of early stationary phase cells using BmtI-cut pLKL67Y containing 4 nt 3' overhangs.....	41
18. Mutation frequencies of various DSB repair pathway mutants.....	42
19. Mutation frequencies of WT and <i>nej1</i> mutants.....	44
20. Mutation frequencies of mutant cells using DSBs with different 4 nt 5' overhangs	45
21. Mutation frequencies of early stationary phase cells using BmtI-cut pRS315URA3.....	46
22. Plasmid repair efficiencies of early stationary phase cells and G ₁ percentages within each cell culture.....	48
23. Plasmid repair efficiencies of true stationary phase cells and G ₁ percentages	50
24. NHEJ repair efficiencies of mid-log phase cells using NcoI-cut pRS315URA3	52
25. Repair efficiencies determined using DSB with 3' and 5' DNA.....	54
26. Similarities between the HR pathway and plasmid with 3' overhangs	55

CHAPTER I

INTRODUCTION

Damage and repair in DNA

In all living cells DNA is constantly bombarded with damaging agents such as DNA nucleases, ionizing radiation, and chemical mutagens (1-3). These agents can cause a variety of different lesions such as modified deoxyribose and bases, crosslinks (both intra- and interstrand), and both single-strand breaks (SSBs) and double-strand breaks (DSBs) (1, 4). Lesions vary in severity and could possibly lead to hindrance of both the transcription and replication machinery, which could eventually lead to further DNA damage, mutations and cell death. Because of this, a variety of repair pathways are necessary for the survival of the cell.

Cells contain distinct repair pathways that employ their own specific protein complexes in order to function. Major repair pathways in eukaryotes include Nucleotide Excision Repair (NER), which repairs damage induced by ultraviolet light (UV) such as thymine dimers, Base Excision Repair (BER), which repairs bases modified due to oxidation, alkylation, and deamination, and Mismatch Repair (MMR), which repairs mispaired nucleotides that occur during DNA replication and recombination (4). Another major form of DNA damage is a double-stranded break (DSB). DSBs can be caused through internal processes inside the cell such as nuclease activity, DNA replication arrest, oxidative damage and can also be caused by exposure to various chemical mutagens as well as to ionizing radiation (1-3). The lethality of DSBs are far greater than other lesions. They are more difficult to repair and even one DSB left unrepaired can

potentially cause loss of cell function, cell death or cancer (5). Because of the severity of DSBs, eukaryotic cells contain two specific pathways for repair: homology directed recombination (HDR), also commonly referred to as homologous recombination (HR), and nonhomologous end-joining (NHEJ) (6-9). Although both pathways repair DSBs, they each use several specific protein complexes that are unique to each pathway. The major proteins involved in each pathway are conserved in both yeast and humans (10).

DSB repair in *Saccharomyces cerevisiae*

The two DSB repair pathways, HR and NHEJ, have been well studied for some time in the budding yeast *Saccharomyces cerevisiae*. Although both pathways are conserved within yeast and humans, HR is the preferred pathway in yeast while NHEJ is the preferred pathway in humans when repairing DSBs (6, 9).

The HR pathway in yeast requires the use of homologous regions of chromosomes or sister chromatids that are similar in sequence to repair DSBs by using them as a template. Two major protein complexes involved in the HR pathway include the Mrx protein complex which is composed of Mre11, Xrs2, and Rad50, and the RAD52 group of proteins including Rad51, Rad52, Rad54, Rad55, Rad57, and Rad59. Both complexes are required to repair DSBs efficiently, with the RAD52 group being involved only in HR and the Mrx complex being present in NHEJ as well (9, 11).

The first step in DSB repair through HR is initiated by the Mrx complex, which creates long 3' ended single-stranded DNA tails that are hundreds of nucleotides long using its nuclease/ helicase activity. Sae2 is also involved in this first step. These single-stranded regions are then expanded by the action of nucleases/helicases Exo1 and Sgs1-

Dna2 (9, 11). The single strands are coated with Rpa (single-stranded DNA binding proteins) and then the Rad52 complex facilitates invasion by the long 3' single-stranded DNA tails into unbroken homologous regions of another chromosome (9, 11). Those homologous regions of the chromosome then serve as a template in a series of poorly understood steps that ultimately lead to highly accurate repair (9, 11). The efficiency of HR repair can be influenced by other cellular processes such as chromatin remodeling/reassembly, sister chromatid cohesion, and DNA damage-responsive cell cycle checkpoints (9).

The second of these pathways is the NHEJ pathway (Figure 1). Unlike HR, this pathway does not require the use of a homologous template DNA, as implied by the name. The NHEJ pathway is initiated by the Ku complex, composed of Yku70 and Yku80 in yeast cells and hKu70 (Xrcc6) and hku80 (Xrcc5) in human cells (6-8). The main functions of this complex are to bind non-specifically to the ends of the DSB strands, preventing any degradation by nucleases, and it also recruits the next NHEJ complex, called Mrx (6-8). The second of the three complexes, Mrx, is composed of Rad50, Mre11, and Xrs2 and binds to the Yku complex as well as the broken DSB ends. Mrx keeps the ends in proximity as well as recruits the third NHEJ complex called DNA Ligase IV (6). DNA Ligase IV, the last of the three complexes, is composed of Dnl4, Lif1 and Nej1, which associates with the two previous complexes and directly ligates the two broken ends, thus completing the NHEJ DSB repair pathway (6). Nej1 also plays other roles such as reactivation of Dnl4-Lif1 after repair along with binding to initial complexes in the NHEJ pathway, thus promoting it as the repair pathway of choice (31).

Repair by NHEJ leads to small mutations at the break site at a higher frequency than repair by HR. Most such mutations are short insertions or deletions.

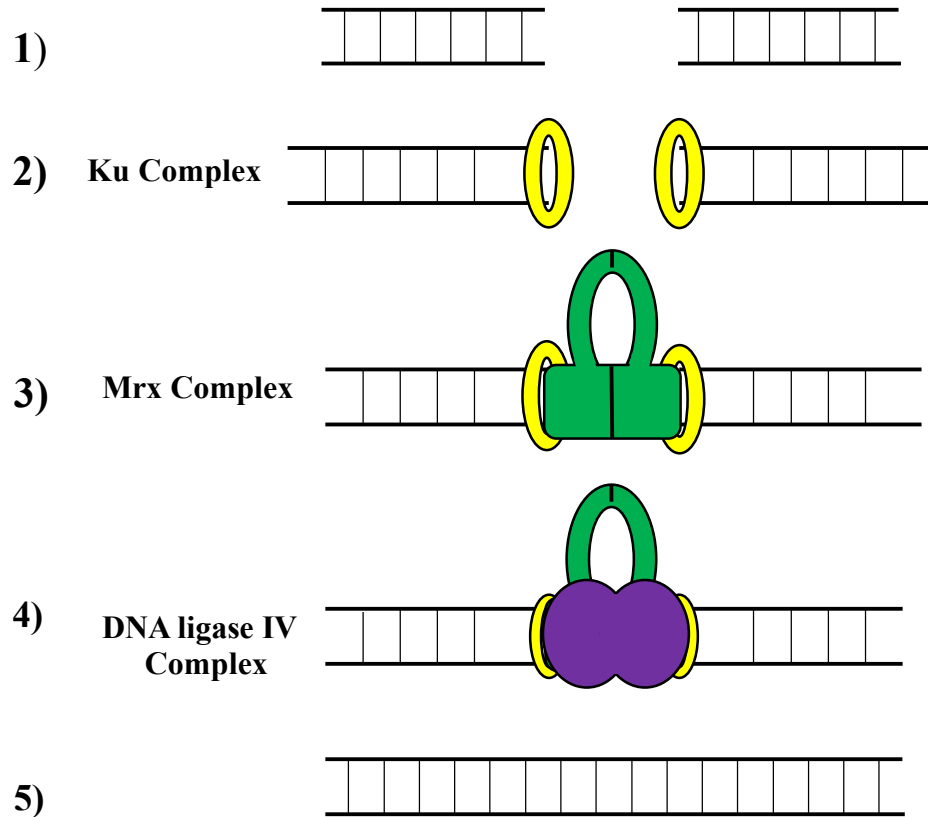


Figure 1. Diagram of NHEJ pathway. NHEJ repair is mediated by 3 major protein complexes.

It is well understood that G_1 phase cells prefer NHEJ as the main pathway for repairing DSBs found within the cell (32-33). This is due to the fact that when a cell is in the G_1 phase there are no homologous sister chromatids present, which is the preferred substrate for HR to repair DSBs. In early stationary phase cell cultures (Figure 2), the G_1 phase percentage is about 60%, while late stationary phase cells have $\geq 90\%$ G_1 phase cells. In contrast, log phase cell cultures have about a $\sim 30\%$ G_1 phase cell count.

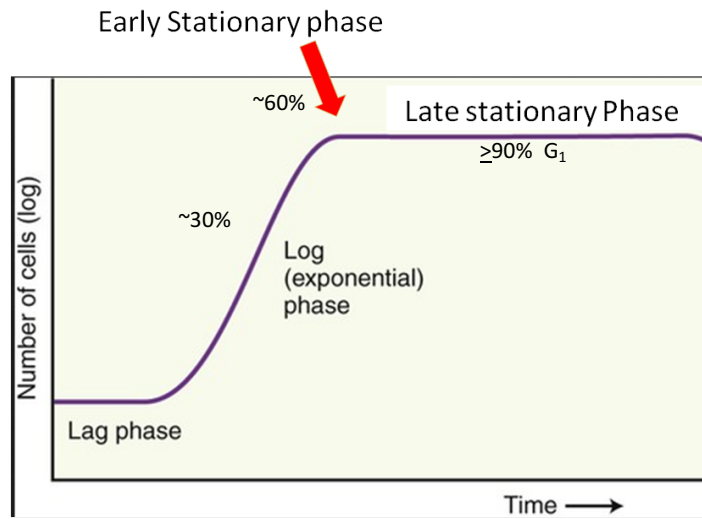


Figure 2. The different levels of G₁ phase cell cultures. Diagram indicating the different G₁ percentages associated with the cell cycle phases. Log phase (~30% G₁) early stationary (~60% G₁) and late stationary (≥ 90% G₁) cells are shown in the figure.

The Yku Complex of *S. cerevisiae*

The Yku complex is a ring-shaped heterodimeric complex that takes part in a variety of different processes other than in NHEJ, such as V(D)J recombination and telomere maintenance (7, 12, 13, 14). A mutation in the hKU70/86 complex, the human homolog, causes severe combined immunodeficiency disease (SCID) also known as bubble boy disease (15). This is due to its role in the V(D)J recombination mechanism in which antibodies in B cells and T cell receptors in T cells are produced (15). Evidence from Porter *et al.*, Boulton *et al.*, and Gravel *et al.* all discuss shortening of telomeres in response to the deletion of either Ku subunit in *S. cerevisiae* cells (12, 16, 17, 18, 19).

Evidence suggests that the Ku complex may be involved in the processing of lesions near the broken ends of the DNA through the activity of its dRP/AP lyase activity (8, 34-38).

The Mrx Complex of *S. cerevisiae*

The subunits making up the Mrx complex are all part of the RAD52 epistasis group that is involved in the HR pathway, and they also function in the NHEJ pathway. Yeast mutants with *MRE11*, *RAD50* or *XRS2* inactivated are defective in not only DSB repair but also in telomere length maintenance and in mitotic and meiotic recombination (20). Although the Mrx complex functions in both HR and NHEJ, it serves two completely different roles. In HR, Mrx is responsible for initiation of nuclease resection activity, but it also plays a role in NHEJ, bringing the two DSB ends in proximity, and recruiting the DNA ligase IV complex (6, 9, 39). The exonuclease activity on dsDNA in a 3'-5' manner is due in part to the Mre11 subunit in which, in HR, makes the initial cut before resectioning in the 3'-5' direction while other nucleases, Exo1 and Sgs1-Dna2 resections in a 5'-3' direction (39, 40). Past studies have suggested that a mutation in the human homolog hMRE11 causes a cerebral degenerative disease ataxia-telangiectasia-like disorder associated with chromosomal instability and increased risk of cancer (21).

The second subunit of the Mrx complex is the Rad50 subunit. Rad50 belongs to the structural maintenance of chromosome (SMC) family of proteins and is an ATPase enzyme (22). The Rad50 subunit is a long fibrous protein and is what stimulates Mre11's nuclease activity (22). It also contains a highly conserved coiled-coil structure known as the RAD50 hook which is believed to mediate the interaction between two Rad50 subunits in the complex. This interaction is essential for creating the DSB proximity function in NHEJ (22, 23).

The third subunit comprising the Mrx complex is the Xrs2 subunit. Xrs2 is responsible for binding the Mrx complex to the DNA in a structurally specific manner (24). It also stimulates Mre11's exonuclease activity as well as interacts with Lif1, one of the subunits present in the DNA ligase IV complex, attracting the complex (24). A mutation in NBS1, the human homolog of Xrs2, is responsible for the disorder known as Nijmegen breakage syndrome, which is associated with chromosomal instability and sensitivity to radiation (25).

The DNA Ligase IV Complex of *S. cerevisiae*

The last of the three complexes found in NHEJ is the DNA ligase IV complex, which is composed of Dnl4, Lif1 and Nej1. Dnl4 is the catalytic subunit of the complex. Lif1 is the subunit responsible for binding to the BRCT domain of Dnl4 and targeting it to DSB ends and to the Xrs2 subunit (26). This interaction is required for alignment/stability and efficiency of Dnl4 ligation of DSBs in NHEJ (26). Studies by Valencia *et al.* have suggested that Nej1 regulates nuclear localization of Lif1, which is responsible for Dnl4 processing and stability (27). Nej1 appears to be involved in both the initial and final steps of NHEJ with evidence suggesting its involvement in stabilizing the binding of the Yku complex to the DSB ends as well as functioning in the nuclear localization of Lif1 in the final step of NHEJ (31). Mutations in human hLIG4 have shown association with LIG4 syndrome, an NHEJ disease that is also an immunodeficiency syndrome like SCID (26).

Measuring NHEJ Repair Efficiency Through Plasmid Assays

Plasmid NHEJ assays are the most common method used for the measurement of NHEJ repair efficiency in yeast cells. The process consists of inducing a DSB with a restriction endonuclease within a plasmid lacking homology with the cell's chromosomal DNA, preventing the initiation of HR and assuring the NHEJ pathway as the pathway used for DSB repair (Figure 2). The DSB in the plasmid also inactivates a gene encoding an enzyme required for the biosynthesis of an amino acid or base such as uracil. After the transformation, the cells are then plated on selective media and grow only when NHEJ repairs the DSB and re-circularizes the plasmid.

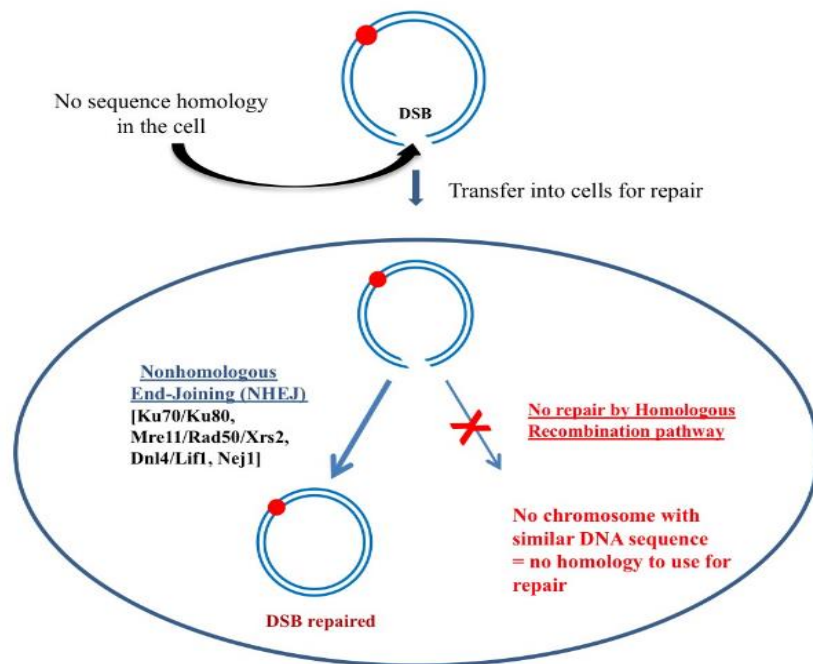


Figure 3. Lack of homology within yeast cell. Depiction of the NHEJ plasmid assay and how repair by HR is impossible, leaving only NHEJ as the main pathway repairing DSBs.

Previous research in other laboratories revealed that mutations in Ku, Mrx, and DNA ligase IV complex genes lead to a near complete inactivation in NHEJ repair

relative to wild type (WT) (Table 1) (28). Experiments done in our laboratory by Whitney Wood have provided preliminary evidence that mutations in the Ku and DNA ligase IV complex have a larger NHEJ repair reduction when compared to a mutation in the Mrx complex. This finding contradicts the work done in other laboratories that suggested that all three complexes are equally important in the pathway, though this conclusion has not been tested rigorously until the current study.

Table 1. Previous studies on NHEJ repair efficiency Previous studies have concluded that all complexes reduce NHEJ repair efficiency approximately equally (28). (+, wildtype level; -, modest defect; ---, severe defect)

Yeast Strain	NHEJ Repair	* Homologous Recombination Repair
<i>Wild Type</i>	+	+
<i>yku70</i>	---	+
<i>yku80</i>	---	+
<i>mre11</i>	---	-
<i>rad50</i>	---	-
<i>xrs2</i>	---	-
<i>dnl4</i>	---	+
<i>lif1</i>	---	+
<i>nej1</i>	---	+

To transform yeast cells with plasmid DNA, cells are typically treated with chemicals in order to increase membrane permeability. The chemicals include

polyethylene glycol (PEG4000), lithium acetate (LiAc), and dimethyl sulfoxide (DMSO) (Figure 3) (29, 30). The cells for transformation are exposed to a heat shock step at 42° C to destabilize membranes further and are then spread to a plate to allow formation of colonies (Figure 3) (29). The Lewis lab developed a new method for transforming overnight cultures of yeast cells (early stationary phase cells) with plasmids that improves the efficiency of the process (29). The major modifications were to add two new steps (shown in red in Figure 3). Cells are pre-treated with the disulfide bond-reducing agent dithiothreitol (DTT), which is capable of disrupting protein structures on the cell surface. In addition, after the heat shock step, the cells are allowed to recover from the chemical treatment in rich YPDA broth. Inclusion of both of these steps increased transformation efficiencies by more than five-fold (29).

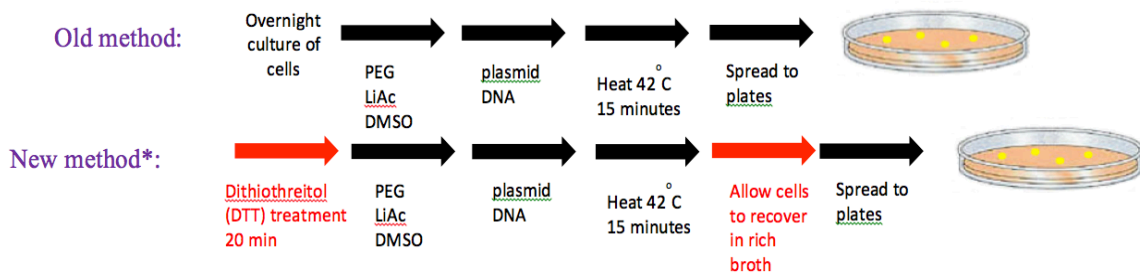


Figure 4. Traditional and modified transformation methods. The steps followed for transformation of yeast cells with plasmids by the traditional method (top pathway) or using the new method developed in this laboratory (bottom pathway) (29).

Measuring Accuracy of Plasmid DNA Repair

After transformation, the plasmid could potentially undergo different outcomes. The repair of the DSB could lead to a mutation near the repair site in the plasmid or the NHEJ pathway could accurately repair the DSB on the plasmid giving the same results as inaccurate repair. In order to differentiate between inaccurate and accurate repair the

plasmid containing two genes would be patched and replicated onto media lacking a specific amino acid or base. If inaccurate repair occurred, the colonies would not grow, but when accurately repaired the gene encoding the specific biosynthetic enzyme would be reinstated, leading the cell to grow in media lacking said amino acid or base.

Goals of research

The goals of this project were to determine the importance of the three major NHEJ complexes (Ku, Mrx, and Dnl4) in DSB repair by the NHEJ pathway using plasmid-based assays. Although past studies have suggested that inactivation of any of the complexes completely inactivates the pathway, preliminary work in this lab suggested that the Mrx complex (Mre11, Rad50, and Xrs2) and the Nej1 subunit of the Dnl4-Lif1-Nej1 complex are not as critical as the other proteins.

The second goal was to test the importance of cell cycle phase (varying G₁ levels) in repair by NHEJ. Past work has indicated that NHEJ is more active in G₁ phase than in the other phases (32). Plasmid NHEJ assays were performed using cell cultures that are either very high (stationary phase) or very low (mid-log phase) in G₁ phase cell percentage. Results suggested that a higher G₁ phase cell percentage showed a lower requirement for the Mrx complex in repair efficiency. In contrast, cultures with a low G₁ phase cell percentage exhibited an equal requirement for all three complexes.

The final goal of this project was to examine the difference in both repair and accuracy in NHEJ mutants (*yku70*, *mre11*, and *dnl4*) when the single-stranded DNA overhangs on a plasmid after digestion were either 5' or 3' sticky ends. The plasmids with 3' overhangs showed equally poor NHEJ repair in *yku70*, *mre11* and *xrs2* mutants,

indicating that all three complexes are required. The plasmids with 5' tails showed strong requirement for the Yku and Dnl4 complexes, but not the end-bridging Mrx complex. As for accuracy, a plasmid containing 4 nt 3' overhangs (BmtI-cut pLKL67Y) was observed to have a high mutation frequency in *mre11* mutants when compared to a plasmid containing 4 nt 5' overhangs (NcoI- and AflIII-cut pRS315URA3), in which *mre11* mutants had a mutation frequency similar to that of WT cells (0%).

CHAPTER II

MATERIALS AND METHODS

1. Materials

General Reagents and Equipment

EDTA was purchased from Omnipur (Darmstadt, Germany). Sonics-Vibra Cell (Newton, CT) supplied the sonicator. Amino acids (leucine, lysine, adenine, uracil, and histidine), lithium acetate (LiAc), dimethyl sulfoxide (DMSO), 10 amino acid mix, ampicillin, and RNase A were all purchased from Sigma-Aldrich Chemical Co. (St. Louis, MO). Fluka Analytical supplied polyethylene glycol – 4000 (PEG). Tris base was purchased from Shelton Scientific, Inc. (Peosta, IA). Ethidium bromide was from IBI Scientific (Peosta, IA). New England Biolabs (Ipswich, MA) supplied 2-log DNA ladder, NcoI, AflII, and BmtI. Dithiothreitol (DTT) and agarose LE were supplied from Gold Biotechnology (St. Louis, MO). Sonicated salmon sperm DNA (10 mg/ml) was provided by Agilent Technologies (Santa Clara, CA). 50X Tris-acetate, and 0.05 M EDTA pH 8.3 were purchased from OMEGA Bio-Tek (Norcross, GA). Avantor (Center Valley, PA) supplied ammonium sulfate. D-Glucose (dextrose), and soy peptone were supplied by VWR (Radnor, PA). Bacto yeast extract was purchased from BD Bioscience (San Jose, CA). Teknova (Hollister, CA) supplied the agar. ThermoFisher (Waltham, MA) supplied the Qubit 2.0 fluorimeter. Alpha Innotech Red imager was purchased from ProteinSimple (San Jose, CA)

Yeast strains and plasmids

All yeast strains that were used for this project were derivatives from BY4742 (*MAT α ura3- Δ 0 leu2- Δ 0 lys2- Δ 0 his3- Δ 1*). Derivative strains are as follows: YLKL857 (*yku70 Δ ::G418^r*), YLKL923 (*yku80 Δ ::G418^r*), YLKL650 (*mre11 Δ ::G418^r*), YLKL649 (*rad50 Δ ::G418^r*), YLKL858 (*dnl4 Δ ::G418^r*), YLKL914 (*lif1 Δ ::G418^r*), YLKL927 (*nej1 Δ ::G418^r*). Plasmids used for all experiments measuring repair efficiency as well as accuracy were pRS315URA3 (*CEN/ARS LEU2 URA3*), pRS313 (*CEN/ARS HIS3*), pRS315 (*CEN/ARS LEU2*), and pLKL67Y (*CEN/ARS HIS3 URA3*).

2. Methods

Gel electrophoresis

Gel electrophoresis was accomplished using 0.8% agarose gels run with 1X TAE (40 mM Tris base, 20 mM acetic acid, 1 mM EDTA) running buffer at ~130 V on Life Technologies Horizon rigs. Staining of the gels was done with 0.5 μ g/ml ethidium bromide (EtBr) for 15 minutes and they were imaged with an Alpha Innotech Red gel imager from ProteinSimple (San Jose, CA)

Early stationary phase yeast cell transformation

One of the three types of plasmid transformations performed was with early stationary phase cells using a modified version of the protocol described by Tripp *et al.* (29). Increased amounts of DNA were used in order to raise transformation colony numbers for mutant strains known for poor transformation uptake efficiencies. For these

assays and all other NHEJ assays, four independent replicate assays were performed per strain. Averages and standard deviations were calculated and shown in the graphs in the results and discussion section. The protocol is as follows:

1. Centrifuge overnight cultures that were shaken in YPDA broth at 5,000 x g for 15 s. Usually, 1.0 mL was used per assay tube.
2. Resuspend the pellet in 400 μ L of 0.1 M DTT and incubate at 42° C for 20 min. (only 8 min for *yku70/80* mutants due to heat sensitivity)
3. Centrifuge cells for 15 s at 5,000 x g and remove supernatant.
4. Add 507 μ L of master mix solution containing: 400 μ L 50% PEG + 50 μ L 1 M LiAc + 10 μ L 50 mM EDTA + 5 μ L 1 M Tris (pH 7.5) + 20-35 μ L deionized water + 5 μ L mg/mL boiled sonicated carrier DNA + 1-10 μ L of plasmid DNAs per assay and vortex to resuspend. Each master mix includes enough volume for all transformations plus one extra assay.
5. Add 56 μ L DMSO and vortex to mix.
6. Incubate at 30°C, shaking, for 15 min.
7. Heat shock at 42° C for 15 min. (8 min for *yku70/80* mutants)
8. Centrifuge cells at 2,500 x g (usually ~10 s) and remove supernatant. (Low speed is used for easier resuspension of the cell pellets in the next step.)
9. Remove supernatant and resuspend cells in 1,000 μ L YPDA by vortexing and incubate, shaking, at 30°C for 40 min to help cells recover from the chemical incursion. After the YPDA growout, centrifuge cells at 2,500 x g for 10 s and remove supernatant.)

10. Resuspend cells in 200-1000 μL deionized water, depending on the strain. Spread 5-150 μL onto selective plates, depending on the strain. For optimum surface coverage during spreading, spot 50 μL of deionized water onto plates receiving 50 μL or less of cells prior to pipetting cells onto the plate.
11. Incubate plates at 30°C for ~ 3 days or at RT for 4-5 days.

Stationary phase yeast cell transformation

For true stationary phase yeast cell transformation, the modified Tripp *et al* transformation protocol was used as before with additional steps to ensure use of 1×10^8 of yeast cells. Cells were grown on YPDA plates for at least 4 days at 30°C to ensure they reached stationary phase. The additional steps are as follows:

1. Using a sterile toothpick, transfer a large mass of cells from multiple colonies of one strain grown on YPDA plates into 400 μL of YPDA broth in microfuge tubes and vortex.
2. Make a 1:100 dilution, vortex and sonicate for 15 seconds at 24% amplitude.
3. Transfer ~ 12 μL onto a hemocytometer and count cells within squares three separate times and average the three counts.
4. Solve for cell titer by multiplying the average by 25 (squares) \times 10,000 (hemacytometer multiplication factor) \times 100 (fold dilution)
5. Divide 1×10^8 (desired cell count) by calculated cell titer then multiply by 1000 to get the number of μL that is equal to 1×10^8 total cells.
6. Add calculated volume into microfuge tubes.

The remainder of the steps follow the modified Tripp *et al.* protocol for early stationary phase transformation.

Mid-log phase yeast cell transformation

The initial steps for the transformation of mid-log phase yeast cells are similar to steps 1-5 of the stationary phase cell transformation with a minor change in the dilution being 1:40 rather than 1:100, and 1.5×10^7 total cells being divided by the average cells/mL calculated from the hemocytometer instead of 1×10^8 . The remainder of the steps are as follows:

1. The calculated volume is added to 10 mL of YPDA broth in a 50 mL screwcap tube with a loosely taped lid and placed in a 30°C shaker for 6 h to reach mid-log phase. The stationary cell titer is 1.5×10^6 cells per mL.
2. After 6 h growth at 30°C, centrifuge cells for 5 min at 3,800 x g and discard the supernatant.
3. Add 1 mL of 0.1 M LiAc, resuspend pellet by vortexing and transfer the cells to a 1.5 microfuge tube.
4. Centrifuge for 15 s at 2,500 x g and discard supernatant.
5. Add 351 μ L of master mix solution containing: 240 μ L 50% PEG + 36 μ L 1 M LiAc + 5 μ L mg/mL boiled sonicated carrier DNA + 70 μ L of (deionized water + plasmid DNA) per assay then resuspend. Each master mix includes enough volume for all transformations plus one extra assay.

6. Shake at 30°C for 20-30 min.
7. Put to 42°C for 8-20 min (*yku70/80* only 8 min).
8. Centrifuge for 15 s at 2,500 x g and remove supernatant.
9. Resuspend cells in 200-1000 µL deionized water, depending on the strain. Spread 5-150 µL onto selective plates, depending on the strain. For equal spreading on the surface of the plate, spot 50 µL of deionized water onto plates receiving 50 µL or less of cells prior to pipetting cells onto the plate.
10. Incubate plates at 30°C for ~3 days or at RT for 4-5 days.

Plasmid DNA midipreps

Ninety mL of overnight cultures of *E. coli* cells containing the desired plasmid were grown in TB + Amp broth shaking at 37°C overnight and 45 mL centrifuged at 17,000 x g for 1 min at 4°C in 50 mL tubes in the Lynx 6000 floor centrifuge. Pellets were then resuspended in 1.5 mL of cold TE (10 mM Tris, pH 8 + 1 mM EDTA pH 8) and 3 mL of freshly made 0.2 M NaOH + 1% SDS and inverted rapidly, followed by a 3 min incubation on ice. Two and a half mL of cold 3 M KOAc was then added to the mixture and it was inverted several times followed by an additional 5 min incubation time on ice. The cells were then centrifuged at 17,000 x g for 15 min and the supernatant was transferred to a new container and DNA was precipitated using isopropanol followed by centrifugation at 17,000 x g for 5 min at 4°C. The supernatant was discarded and the pellet was washed with 70% cold ethanol for 1-2 min. Tubes were inverted on Kimwipes to dry for a minimum of 60 min. Once dried, the pellet was resuspended in 0.8 mL TE +

10 μ L of 1 mg/mL RNase A and incubated on ice for greater than or equal to 10 min. The solution was then transferred to a microfuge tube and stored at -20°C .

Plasmid DNA digestion

pRS315URA3 was digested using the restriction enzyme NcoI (10,000 U/mL) to create a DSB in the *URA3* gene. Typical reactions involved 30 μ L of plasmid DNA, 235 μ L deionized water, 30 μ L 10X NEB 3.1 buffer, and 3 μ L of NcoI (300 units) followed by an incubation time of 5-6 h at 37°C . After incubation, the digested plasmid was ethanol precipitated with the addition of $1/20^{\text{th}}$ volume of 3 M NaOAc followed by 2.5 volumes of cold 100% ethanol and left to incubate for 15 min on ice. The DNA was centrifuged for 15 min at 21,000 x g and the supernatant was discarded and then 300 μ L of 70% ethanol was added and the tube was centrifuged again for 2 min at 21,000 x g. After the supernatant was discarded, the DNA pellet was placed in a Thermo Scientific Savant DNA 120 Speedvac Concentrator for 10 min to dry. Once dried, the pellet was resuspended in 150 μ L of deionized water, vortexed, and left to sit for a minimum of 5 min. The DNA digestion was analyzed using a 0.8% agarose gel in order to confirm a successful digestion. The concentration of the digested DNA was measured using a Life Technologies Qubit 2.0 Fluorimeter in accordance with the manufacturer's protocol. The digestion was then stored at -20°C for later use. The same procedure was used for an AflII restriction enzyme digestion of pRS315URA3 and the digestion of pLKL67Y using BmtI, using the appropriate buffers required for each reaction.

Nonhomologous end-joining efficiency assays

The majority of the mutants were transformed using NcoI-cut pRS315URA3 DNA (100 ng per transformation) using the Tripp *et al.* protocol (29). The uncut plasmid pRS313 (100 ng per transformation) was simultaneously transformed in order to calculate transformation efficiency as a control. For every NHEJ test, 1 mL of cells were put into 4 separate assay microfuge tubes with WT (BY4742 *MAT α*) as the control for each experiment. All strains used were Ura⁻, Leu⁻, and His⁻ with the cells only becoming His⁺ when pRS313 plasmid was successfully transformed, Leu⁺ when cells took up and recircularized NcoI-cut pRS315URA3, and Leu⁺ Ura⁺ when NcoI-cut pRS315URA3 plasmid was accurately repaired. To calculate repair efficiencies, the transformants were spread accordingly onto glucose minus leucine (Glu-Leu) and glucose minus histidine (Glu-His) plates. Colonies that were counted on Glu-Leu plates represented cells that repaired NcoI-cut pRS315URA3 while colonies counted on Glu-His plates represented cells that successfully transformed pRS313. Repair efficiencies were normalized to transformation efficiencies by dividing the number of Leu⁺ transformants per μg of DNA by the number of His⁺ transformants per μg of DNA.

This same process was also done to other cut plasmids. For AflII-cut pRS315URA3 in which the *LEU2* gene was cut, transformants were spread onto glucose minus uracil (Glu-Ura) plates while still using uncut pRS313 as a control. For BmtI-cut pLKL67Y transformation, in which the *HIS3* gene was cut, transformants were spread onto Glu-Ura plates and uncut pRS315 was used as a control and spread onto Glu-Leu plate.

Nonhomologous end-joining accuracy tests

To test NHEJ repair accuracy, colonies that grew on Glu-Leu plates that had repaired NcoI-cut pRS315URA3 were patched onto fresh Glu-Leu plates and grown for 2 days at 30°C. These plates were then replica plated to Glu-Leu and Glu-Ura plates to identify Ura⁻ cells. Colonies that grew on both Glu-Leu and Glu-Ura plates had accurately repaired the DSB caused by NcoI in the *URA3* gene of the pRS315URA3 plasmid. This same method was also used for plasmids containing other restriction enzyme cuts such as AflIII-cut pRS315URA3, with accurately repaired cells growing on Glu-Leu plates, and for BmtI-cut pLKL67Y, with accurately repaired cells growing on Glu-His plates. For each strain, greater than or equal to one hundred colonies were patched and replica plated to determine accuracy.

Analysis of cell cycle phases

Unbudded, small-budded and large-budded cells were counted using a United Scope model M837 phase contrast microscope (Hopewell Junction, NY) using a hemacytometer. Unbudded cells corresponded to G₁ phase cells. Small-budded S phase cells were distinguished from large-budded G₂/M cells using the following rule: If the largest diameter of the bud was greater than or equal to 50% of the largest diameter of the mother cell, the cells was scored as large-budded. For each replicate, one hundred total cells were counted for two to three replicates of each strain.

CHAPTER III

RESULTS AND DISCUSSION

The aims of this project were to map out the importance of the three major NHEJ pathway complexes (Ku, Mrx, and DNA ligase IV) via plasmid-based assays (8). In this project, all eight genes encoding proteins in the three complexes of NHEJ were tested for their role in DSB repair. Both NHEJ repair efficiencies and accuracies were analyzed through a modified plasmid transformation assay. Another aim of this project was to analyze repair of DSBs with different end structures. DSBs containing either 4 nt 5' ssDNA overhangs or 3' ssDNA overhangs were employed to measure both repair efficiency and accuracy. The genes examined were *YKU70* and *YKU80* comprising the Ku complex, *MRE11*, *RAD50* and *XRS2* encoding proteins of the Mrx complex, and *DNL4*, *LIF1* and *NEJ1*, which encode subunits of the DNA ligase IV complex. The roles of all eight genes involved in NHEJ have never previously been examined in one study.

Assays were performed by using a modified version of the transformation protocol of Tripp *et al.* (20) using a plasmid induced to have a DSB with a restriction endonuclease. This transformation method contained an additional DTT treatment step for higher membrane permeability in the beginning, as well as a YPDA broth grow out

step at the end for cell recovery. These two steps as well as changes in incubation and centrifugation times were used to increase the transformation efficiencies of overnight cell cultures (early stationary phase cells) tested in this project.

The majority of the NHEJ assays done in this project used the plasmid pRS315URA3 (Figure 5). This plasmid contains the yeast *LEU2* and *URA3* genes plus a centromere and origin of replication (ARS). In order to measure repair, a DSB in the *URA3* gene was created by digestion of the plasmid using the restriction enzyme NcoI.

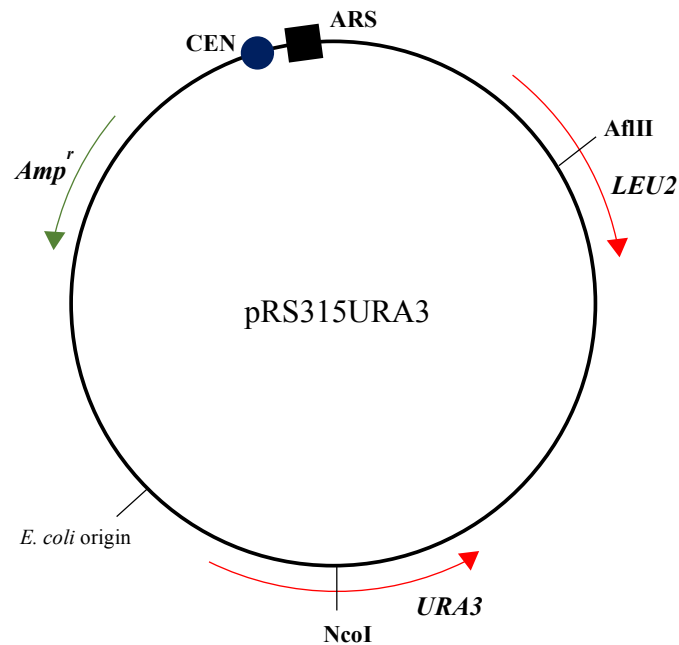


Figure 5. Diagram of the plasmid pRS315URA3. pRS315URA3 contains an AflIII restriction site in the *LEU2* gene and an NcoI restriction site in the *URA3* gene. These sites were used to create linear plasmids containing a single DSB.

An example of the results of this digestion is shown in Figure 6. The gel shows uncut pRS313 plasmid (lane 2), the supercoiled and nicked open circular DNAs of uncut pRS315URA3 (lane 3) and to the linear form (lane 4).

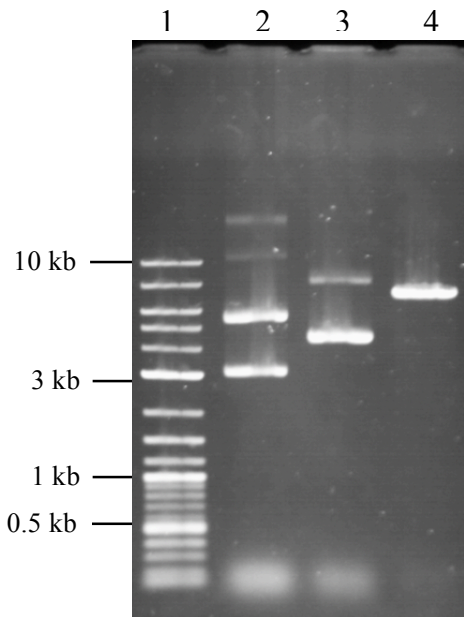


Figure 6. Agarose gel electrophoresis (0.8%) of NcoI-cut and uncut pRS315URA3. Lane 1, 2-Log DNA ladder; Lane 2, uncut pRS313; Lane 3, uncut pRS315URA3; Lane 4, NcoI-cut pRS315URA3.

The two genes present in pRS315URA3 (*LEU2* and *URA3*) play a vital role in the measurement of efficiencies and accuracies. After disruption of the *URA3* gene, via NcoI restriction enzyme, plasmids that are properly transformed and repaired by NHEJ will produce the enzyme encoded by *LEU2*, giving the yeast cells the ability to grow on glucose plates lacking leucine (Glu-Leu). Although a repaired plasmid would produce

Leu⁺ yeast cells, it does not mean the repair was accurate (Figure 7). Leu⁺ yeast cells were patched and replica plated onto both Glu-Leu and glucose minus uracil (Glu-Ura) plates. Cells that grew on both plates had accurate repair through NHEJ, making them Leu⁺ and Ura⁺, while cells that only grew on the Glu-Leu plates were inaccurately repaired making them Leu⁺ Ura⁻ (Figure 7). Cells were also transformed with uncut pRS313 plasmid carrying a *HIS3* gene as a control. The use of two plasmids during transformations, cut and uncut, allowed the measurement of the DSB repair efficiency as a ratio of cut/uncut plasmid. This was done in order to normalize the repair efficiency to the transformation efficiency of each mutant strain that was tested.

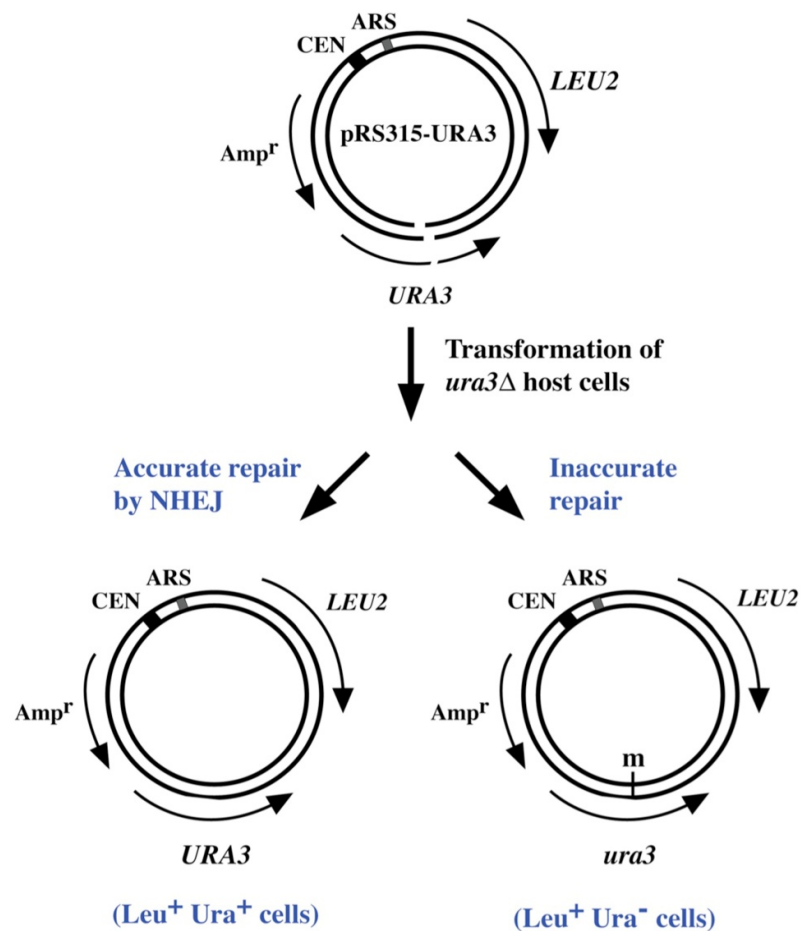


Figure 7. Accurate and inaccurate repair of plasmids. Two possible outcomes after transformation of a DSB-containing plasmid are shown: accurate repair and inaccurate repair leading to a mutation near the site of the break. m, mutation.

Preliminary work done by former student Whitney Wood suggested that *mrx* mutants (e.g., *mre11* strains) are not defective in repair of plasmid DSBs containing 4 nt 5' overhangs, but *yku* and *dnl4* mutants are severely defective. This result contradicts past studies suggesting that all three complexes are required for repair by NHEJ.

Initial experiments for the current project were done with early stationary phase *S. cerevisiae* cells using the transformation protocol used by Whitney Wood but with modifications in microcentrifuge speed, DNA concentrations, and incubation times. A total of 100 ng of the NcoI-cut plasmid pRS315URA3 along with 100 ng uncut pRS313 were transformed into four cell cultures of *S. cerevisiae* BY4742 *MATa* cells (WT) as well as cells that have a deletion of the DNA ligase IV gene *DNL4* in order to measure transformation efficiencies and compare the results to Whitney Wood's preliminary data. Figure 8 shows the results of one of the initial experiments. The fold reduction of 109X seen in this experiment is typical of results that were observed consistently with *dnl4* mutants using NcoI-cut plasmid DNA. This result set a baseline fold reduction that would later be able to be replicated and used as a control throughout the entirety of the project. The results confirm that *DNL4* plays a critical role in NHEJ repair.

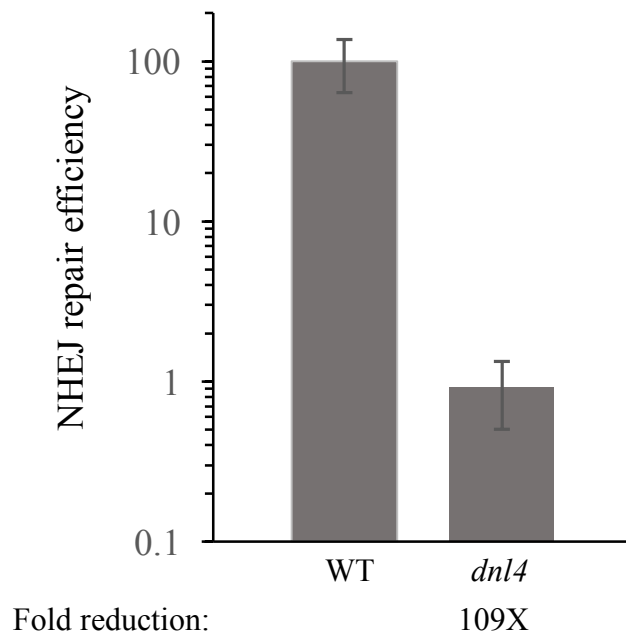
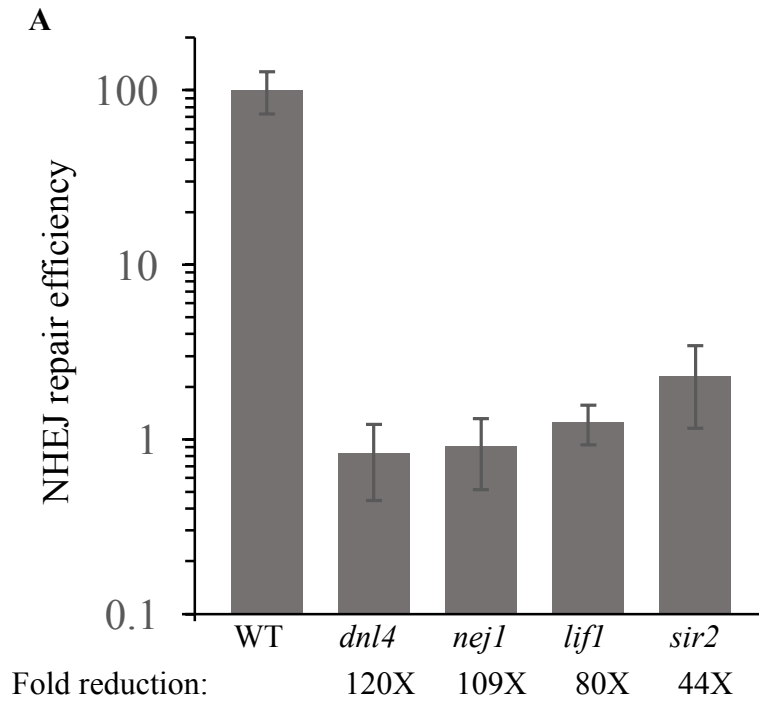


Figure 8. Differences in NHEJ efficiencies of early stationary phase *S. cerevisiae* cells. Both WT and *dnl4* cells were tested. A large reduction was observed in NHEJ efficiency. Four cell cultures were tested for each strain and the results were averaged. Error bars represent standard deviations in this graph as well as all others.

Each complex of the NHEJ pathway was then tested with individual mutants in order to (a) map out the requirement for each subunit according to the complex it functions in, and (b) to be able to select a specific subunit as an established representative of its entire complex (e.g., using *yku70* cells as a representative for the Yku70/80 complex) without risking the possibility of one subunit in the same complex playing a more or less significant role in NHEJ repair efficiency than others. These standards were

established by measuring the reduction in NHEJ repair efficiencies that each mutant individually had when transformed with NcoI-cut pRS315URA3 and uncut pRS313.

The first of the three complexes tested was the DNA ligase IV complex composed of Dnl4, Nej1, and Lif1. This complex is responsible for the ligation of the DSB ends and is the final complex in the NHEJ repair pathway (26). Due to its function in ligating the DSB ends together it is assumed that its role is of high importance when repairing DSBs through NHEJ. The fold reductions in NHEJ repair efficiency were 120X for *dnl4*, 109X for *nej1*, and 80X for *lif1* cells (Figure 9). This result indicates that inactivation of any one of the genes inactivates the whole complex and produces a severe defect in NHEJ. Figure 9B highlights the step in the pathway that was analyzed in this experiment. Figure 9A also shows the NHEJ repair efficiency of mutants with a deletion of the *SIR2* gene. Inactivation of *SIR2* is known to reduce expression of Nej1 protein and is expected therefore to reduce NHEJ repair (41). As shown in the figure, repair was decreased by 44 fold in the *sir2* mutants.



B

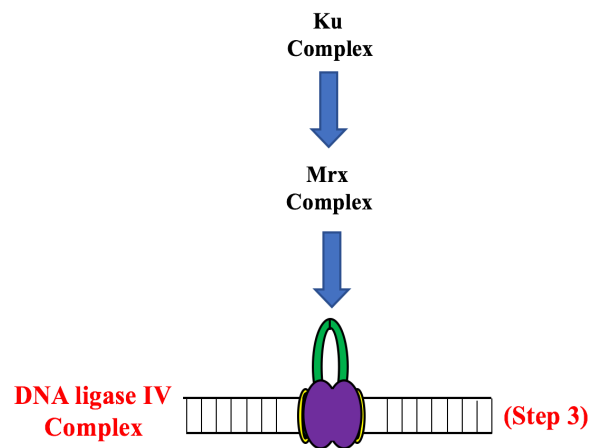
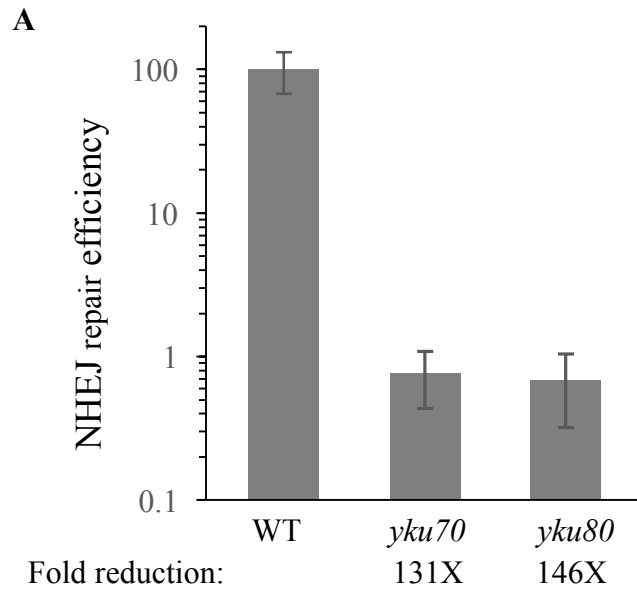


Figure 9. NHEJ efficiencies of early stationary phase cells lacking subunits of the DNA ligase IV complex. Mutants involved in the DNA ligase IV complex have a range of 44-109 fold reductions in NHEJ efficiency. (B) Representation of the step in the NHEJ pathway being tested, which involves ligation of the DSB ends by the DNA ligase IV complex.

The next set of experiments tested the repair efficiencies of Ku complex mutants with deletion of *YKU70* or *YKU80*. The parameters for this transformation were all the same with a slight difference in incubation time during the 42°C DTT treatment (8 min instead of 20 min) and during the 42°C heat shock (8 min instead of 15 min). This was due to the fact that inactivation of the Ku complex in *S. cerevisiae* cells results in heightened heat sensitivity over periods of time longer than 8 min which could lead to cell death (6, 41, 43). A total of 100 ng of plasmid DNA, both NcoI-cut pRS315URA3 and uncut pRS313, was transformed into WT, *yku70*, and *yku80* cells. The function of the Ku complex is to bind sequence-independently to the broken ends of the DSB in order to protect the ends from any potential nuclease degradation and to recruit Mrx and Dnl4 (8, 34-38). Inactivation of the Ku complex could result in the degradation of the DSB ends of pRS315URA3 and failure to recruit other NHEJ proteins after transformation, potentially causing a severe loss of repair efficiency in the NHEJ pathway. *yku70* mutants exhibited a 131 fold reduction in repair efficiency and *yku80* mutants were down 146 fold. These results demonstrated that the subunits of the Ku complex (Yku70 and Yku80) are as critical for NHEJ repair as the subunits of the DNA ligase IV complex (Dnl4, Lif1, and Nej1) (Figure 9).



B

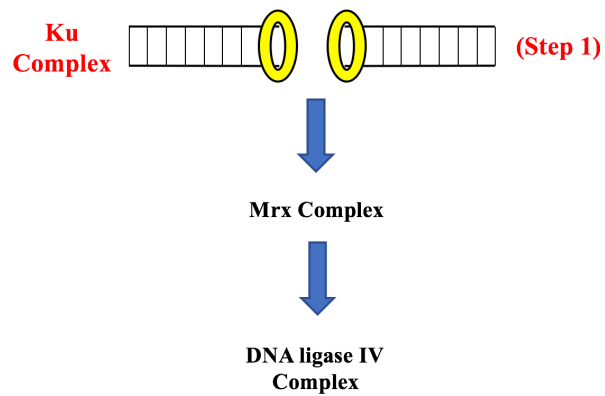


Figure 10. NHEJ repair efficiencies of early stationary phase cells with mutations in Yku complex genes. Repair in *yku70* and *yku80* mutants was reduced ~131-146 fold. (B) Representation of the step in the NHEJ pathway involving the Ku complex.

The third of the three major complexes tested was the Mrx complex, composed of Mre11, Rad50 and Xrs2. The role the Mrx complex plays in the NHEJ repair pathway has been suggested to be the tethering of the two DSB ends, maintaining them close in proximity after the Ku complex binds, as well as in recruitment of the DNA ligase IV complex (6, 9, 24). NHEJ repair efficiencies in *mre11* cells were reduced 2.3 fold, there was a 2.6 fold reduction in *rad50* cells and a 1.2 fold reduction was seen in *xrs2* mutants (Figure 11A). These results are drastically different when compared to reductions observed in both the Ku complex and DNA ligase IV complex mutants, suggesting a less significant role in NHEJ repair in plasmid-based assays. The function of this complex could be critical in chromosomal DSB repair *in vivo* because of the DNA's massive length potentially causing the DSB ends to drift far away from each other. In plasmid assays the potential distance over which the two broken ends can be separated is much smaller than that of chromosomal DSB ends, and its role may not be as critical. These results contradict the current consensus that each complex has equal significance in the NHEJ repair pathway.

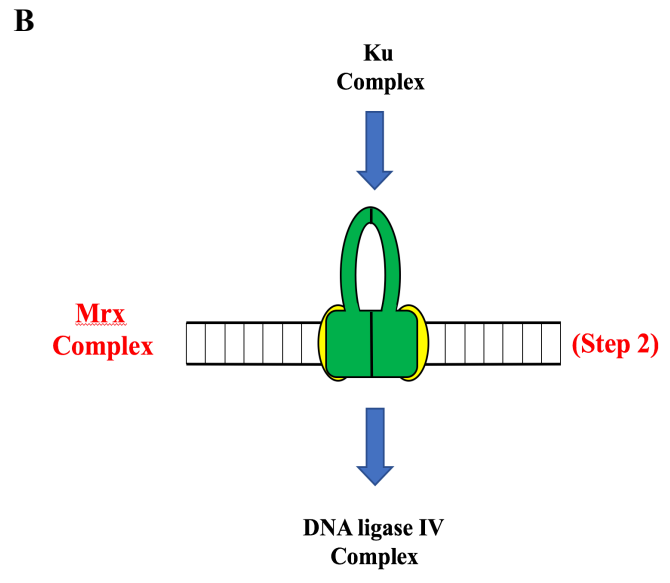
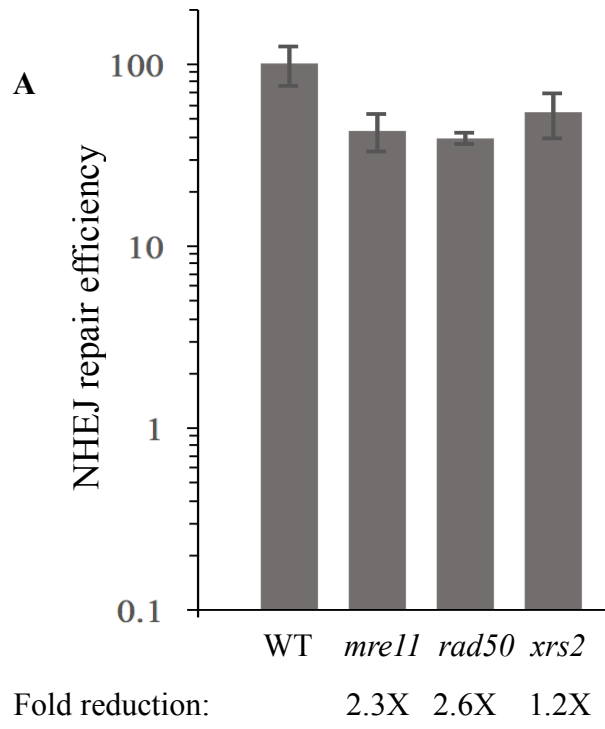
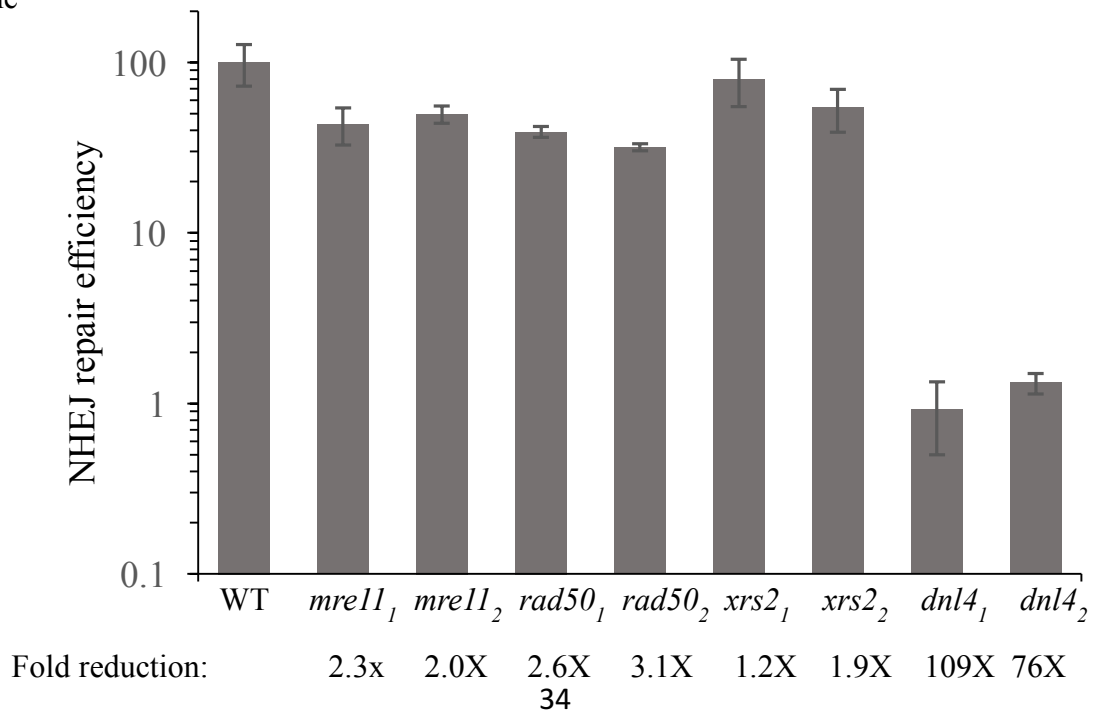


Figure 11. NHEJ efficiencies of early stationary phase mutants lacking components of the Mrx complex. Mutants involved in the Mrx complex of the NHEJ pathway have a range of ~1.2-2.6 fold reductions in NHEJ efficiency suggesting a less critical role in the NHEJ plasmid repair assay when compared to the DNA ligase IV and Yku complexes. (B) Representation of the Mrx complex step in the NHEJ pathway.

In order to determine if the reductions measured in the previous assays of *mrx* mutants were able to be replicated, they were repeated. Figure 12 shows the comparison of repair efficiencies from Figure 11 versus those seen in the duplicate NHEJ plasmid assays. Subscripts in the Figure indicate the first assay (e.g., *mre11*₁) or the second assay (e.g., *mre11*₂). All of the *mre11*, *rad50* and *xrs2* mutant assays showed small reductions ranging between 1.2 and 3.1 fold. These results are in contrast to results of the two separate assays done using *dnl4* mutants, which showed reductions of 109 and 76 fold, respectively. Although the test with *dnl4*₂ resulted in a 76 fold reduction as opposed to the



108.9 fold reduction of *dnl4₁*, the level of reduction, when compared to the Mrx complex reductions, was still much higher. Figure 12 confirms that the Mrx complex does indeed have a much less important role than the Yku and DNA ligase IV complexes.

Another goal of this project was to determine whether there is a difference in NHEJ repair efficiency of DSBs having 5' vs 3' overhangs. Since inactivation of the subunits involved in each of the three NHEJ repair pathway complexes produced similar results (e.g., *dnl4*, *lif1*, and *nej1* mutants all gave similar results), a representative subunit of each complex was able to be chosen without risking one subunit having a more or less significant role than the other within the same complex. The *yku70* mutant was chosen to represent the Ku complex, an *mre11* mutant was chosen for the Mrx complex, and *dnl4* was chosen for the DNA ligase IV complex.

Figure 12. NHEJ efficiency tests of early stationary phase cells containing inactivated Mrx complex genes. Two independent NHEJ efficiency assays on mutants lacking the Mrx complex continued to show small reductions.

The initial transformation experiments described previously all used the NcoI-cut pRS315URA3 plasmid, which contained a DSB with 4 nt 5' ended overhangs (Figure 13). New experiments were performed that involved digestion of plasmids with other enzymes that produced ends that were similar to NcoI or that contained 3' overhangs. The enzymes used were AflIII and BmtI (Figure 13).

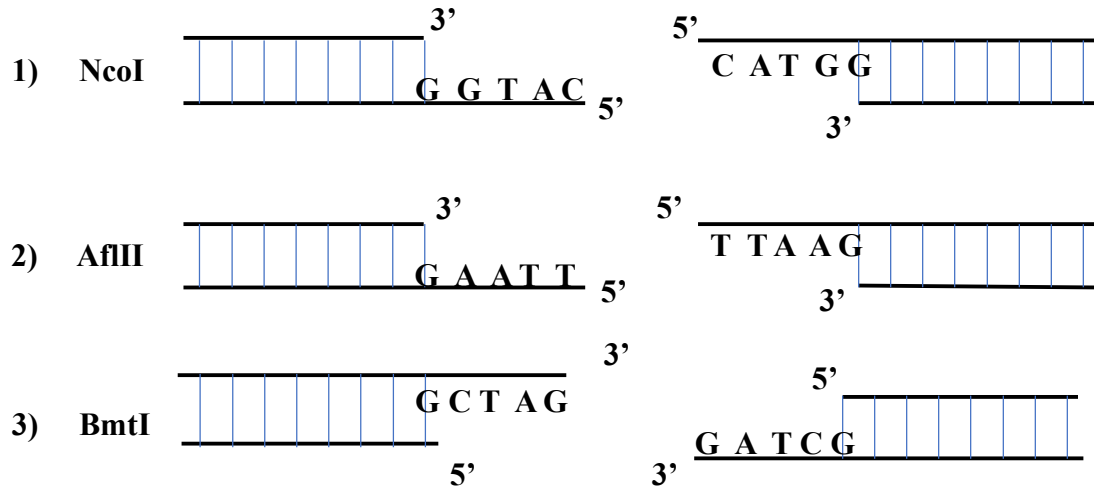


Figure 13. Overhangs produced by digestion of plasmids with the three restriction enzymes used in this study. Digestion of pRS315URA3 plasmid using NcoI or AflIII restriction enzymes leave a 5' overhang while digestion of pLKL67Y plasmid by restriction enzyme BmtI leaves a 3' overhang.

In order to determine if the NHEJ repair efficiencies measured using NcoI-cut pRS315URA3 were replicable using a plasmid also containing a 5' overhang after digestion, but with a different sequence, the same pRS315URA3 plasmid was digested using the restriction enzyme AflIII. Just like NcoI, AflIII leaves a 5' overhang after digestion, but rather than disrupting the *URA3* gene through a DSB, AflIII creates a DSB in the *LEU2* gene (Figure 5 and Figure 13). This meant that, the transformants would be spread onto Glu-Ura plates instead of Glu-Leu plates as previously done. Figure 14

depicts an example of uncut pRS315URA3 plasmid (lane 2) that was run alongside two NcoI-cut pRS315URA3 plasmid digests (lanes 3 and 4) and an AflII-cut pRS315URA3 digest (lane 5). The gel indicates that all of the plasmid DNA was converted to the linear form. A total of 100 ng of the AflII-cut pRS315URA3 plasmid along with 100 ng uncut pRS313 were transformed into WT, *yku70*, *dnl4*, and *mre11* cells to measure NHEJ repair efficiencies and compare them to the results with NcoI-cut pRS315URA3.

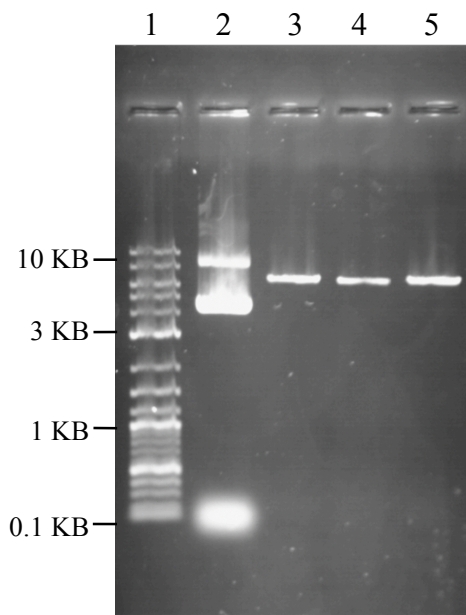


Figure 14. Agarose gel electrophoresis of NcoI-cut and AflIII-cut pRS315URA3.
 A 0.8% agarose gel was used. Lane 1, 2-Log DNA ladder; Lane 2, Uncut pRS315URA3; Lanes 3 and 4, NcoI-cut pRS315URA3; Lane 5, AflIII-cut pRS315URA3.

NHEJ repair efficiencies were reduced 227 fold in *yku70* cells and 116 fold in *dnl4* cells (Figure 15). In contrast, repair in *mre11* mutants was only decreased 2.9 fold. Comparatively, NcoI- and AflIII-cut DNAs both gave ~100 fold reduction in *yku70* and *dnl4* mutants but only 2-3 fold reductions in *mre11* mutants. These results indicate that a plasmid digested with another restriction enzyme leaving a 5' overhang with a different sequence gave essentially the same lack of dependence on Mrx that was seen with NcoI-cut DNA.

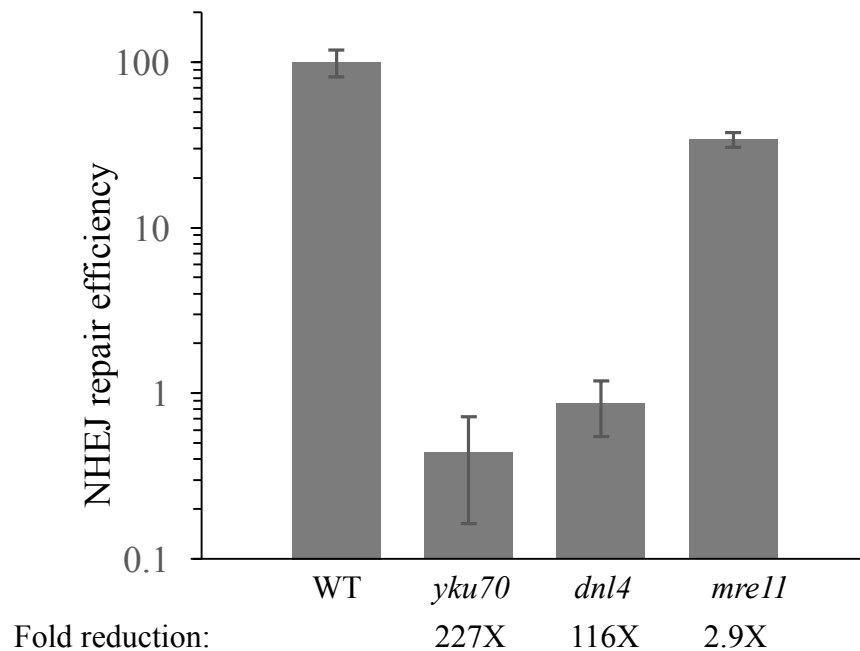


Figure 15. NHEJ efficiencies of early stationary phase cells using a 5' overhang-containing DSB in AflII-cut pRS315URA3. Mutants representing all three complexes (*yku70*, *mrx*, and *dnl4*) were transformed using a plasmid digested using the restriction enzyme AflII, which leaves a 5' overhang similar to the NcoI digested plasmid.

The next test was to digest a plasmid that resulted in a 4 nt long 3' overhang in order to transform cells and measure NHEJ repair efficiencies. There were no known restriction sites that were suitable in either the *LEU2* or *URA3* gene on pRS315URA3 and therefore a new plasmid was chosen, pLKL67Y. The new plasmid contained both a *HIS3* and a *URA3* gene and had a unique restriction site in the *HIS3* gene that could form a DSB with a 3' overhang using the restriction enzyme BmtI (Figure 16A).

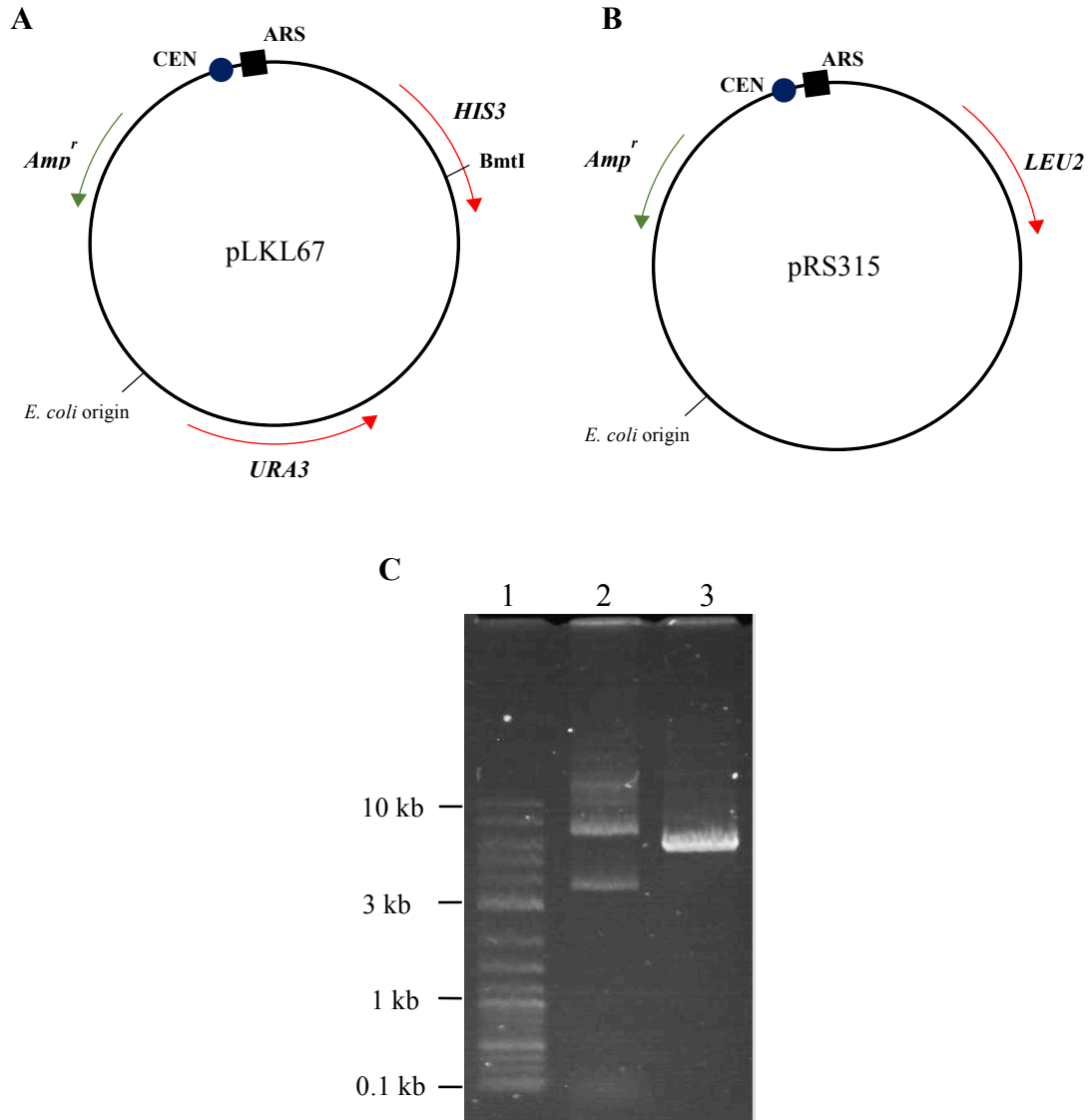


Figure 16. pLKL67Y and pRS315 plasmids. (A) pLKL67Y contains a *BmtI* restriction site in the a *HIS3* gene used to create DSB with a 3' overhang for measurement of repair efficiency. (B) pRS315 was used as a control for transformation efficiency. (C) 0.8% agarose gel. Lane 1, 2-log DNA ladder; Lane 2, Uncut pLKL67Y; Lane 3, *BmtI*-cut pLKL67Y.

The pLKL67Y plasmid was digested using *BmtI*, creating linear pLKL67Y DNA (Figure 16C). An amount of 100 ng of *BmtI*-cut pLKL67Y, for measurement of NHEJ

repair efficiency, along with uncut pRS315 (depicted in Figure 16B) as the control for transformation efficiency, were transformed into WT cells and *yku70*, *dnl4*, and *mre11* mutants. Figure 17 shows the effects on NHEJ repair. *yku70* cells showed a 32.8 fold reduction, *dnl4* cells were down 18.4 fold, and *mre11* cells were reduced 13.4 fold. These reductions were different from those observed using a 5' ended overhang since in this case the requirements for each complex were similar. Although repair was highest in the *mre11* cells, the standard deviation error bars for this strain overlapped those of *dnl4* cells, indicating that they were not statistically different. This result suggests that in an NHEJ plasmid repair assay, the Mrx complex plays a more significant role, approximately equal to the other two complexes, when 3' overhangs are present.

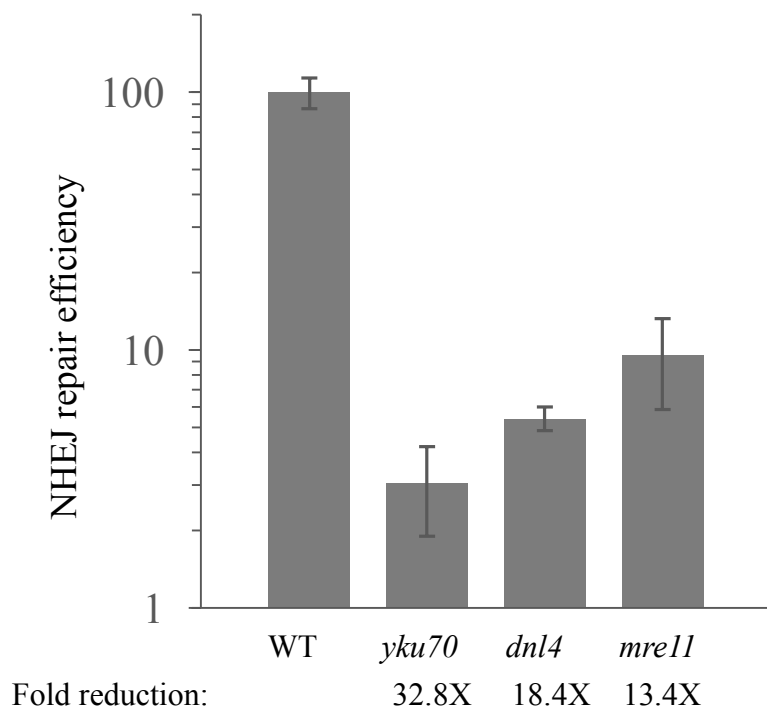


Figure 17. NHEJ efficiencies of early stationary phase cells using BmtI-cut pLKL67Y containing 4 nt 3' overhangs. Mutants representing all three complexes (*yku70*, *mrx*, and *dnl4*) were transformed using a plasmid digested with BmtI, which leaves a 3' overhang different from the NcoI and AflII digested plasmids.

After measuring the NHEJ repair efficiencies, the next objective of the project was to determine accuracies of NHEJ repair in the mutant cells. Past studies have shown that repair by NHEJ in some mutants is highly error prone, producing small insertions or deletions at the junction of the rejoined ends (8, 24, 41, 43, 44). As stated before, the plasmids used for each repair efficiency experiment had to contain two genes, one for the induction of a DSB via restriction enzyme (e.g., in the *URA3* gene in Figure 7). A repaired pRS315URA3 plasmid always makes the cells *Leu*⁺ because of the *LEU2* gene, but then repaired plasmids could be either *URA3*⁺ or *URA3*⁻ depending on whether repair of the DSB was accurate or inaccurate (Figure 7). This means that cells with accurately

repaired NcoI-cut pRS315URA3 plasmid would grow on both Glu-Leu and Glu-Ura plates. However, cells with plasmids that had acquired a mutation in *URA3* would grow on Glu-Leu plates but not on Glu-Ura plates. Former student Whitney Wood measured the accuracy of NHEJ in several mutant strains involved in both NHEJ and HR using the NcoI-cut pRS315URA3 plasmid. Transformed colonies that were Leu⁺ were replica plated to Glu-Ura plates in order to see which were Leu⁺ Ura⁺ versus Leu⁺ Ura⁻. Her raw data has been compiled and converted into the graph in Figure 18. In the graph, the mutation frequency for each strain is expressed as the number of Ura⁻ colonies divided by the total number of Leu⁺ transformants that were tested, normalized to 100%.

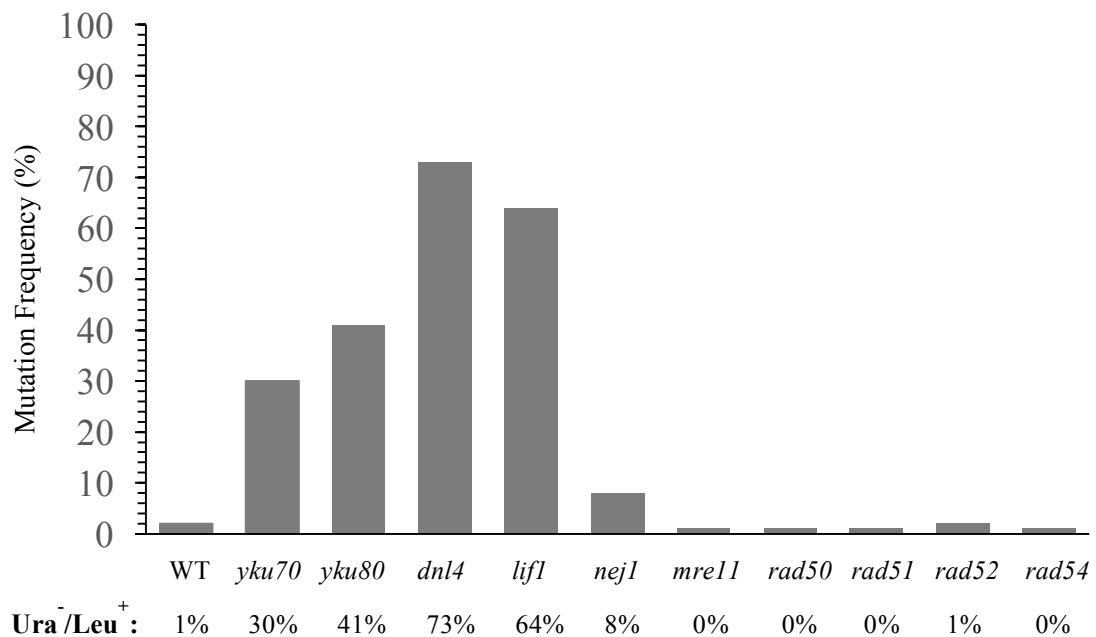


Figure 18. *URA3* gene mutation frequencies of various DSB repair pathway mutants. Previous work done by Whitney Wood allowed calculation of mutation frequencies of several repair-deficient strains.

The results in Figure 18 provide evidence that Mrx complex mutants (*mre11* and *rad50*) are able to accurately repair the DSB in NcoI-cut pRS315URA3 with a mutation

frequency that is similar to the 1% error frequency seen in WT cells. On the other hand, mutants of the Ku complex (*yku70* and *yku80*) and the DNA ligase IV complex (*dnl4* and *lif1*) were highly error prone, with mutation frequencies ranging from 30-73%. As expected, the mutant strains deficient in only the HR pathway (*rad51*, *rad52*, and *rad54*) had WT mutation frequencies due to their lack of function in the NHEJ repair pathway. In contrast to the rest of the DNA ligase IV mutants (*dnl4* and *lif1*), *nej1* cells had a lower mutation frequency, meaning its accuracy in NHEJ repair was greater than the rest of the complex subunits (8% mutations vs 64% and 73%) (Figure 18). Further tests involving mutation frequencies were done to see if the modest effect seen in *nej1* mutants was reproducible. New accuracy tests were performed in WT and *nej1 MAT α* strains, as well as in WT and *nej1 MAT α* strains. As shown in Figure 19, *MAT α nej1* cells again showed only a small increase in mutation frequency (7%), and this was also seen in the *MAT α nej1* mutants (4%). These results confirm that NHEJ repair in *nej1* mutants in other DNA Ligase IV mutant (*dnl4* and *lif1* strains).

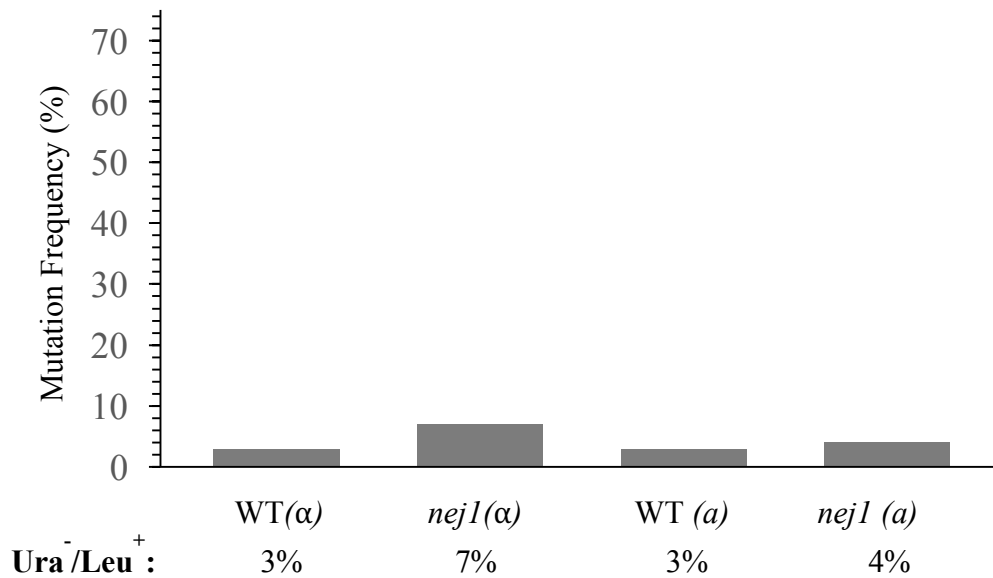
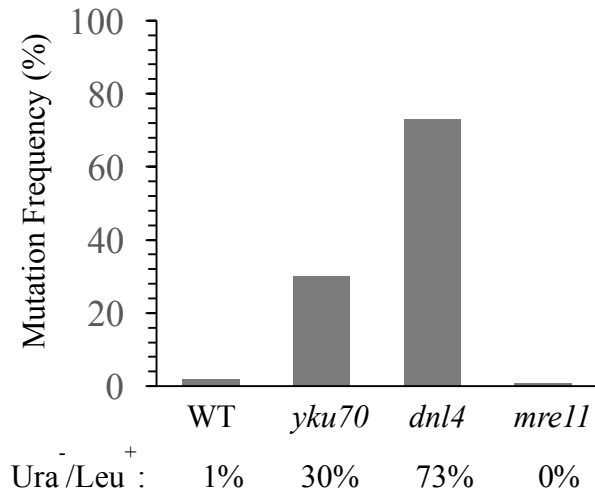


Figure 19. Mutation frequencies of WT and *nej1* mutants. The mutation frequencies of both *nej1a* and *nej1α* cells were similar to each other but different from *dnl4* and *lif1* mutants.

As described previously in order to observe the effect of having 5' overhangs with a different sequence from that of NcoI, pRS315URA3 was digested using AflIII. This created 4 nt 5' overhangs that are the same length but have a different sequence than NcoI (Figure 13). This created a DSB in the *LEU2* gene rather than the *URA3* gene (Figure 5). Figure 20 shows a comparison between mutation frequencies seen with NcoI (Figure 20A) and AflIII (Figure 20B). Although containing different sequences, both cut DNAs had similar mutation frequencies with *yku70* and *dnl4* mutants having high error frequencies (up to 73%) and *mre11* mutants having approximately WT error rates. This suggests that the accuracies of repair of DSBs with 4 nt 5' overhangs is sequence independent.

A



B

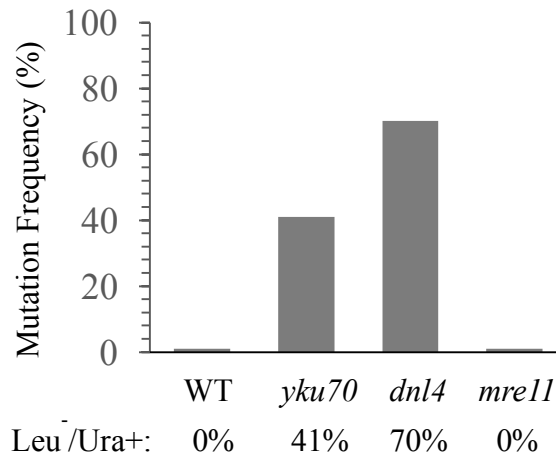


Figure 20. Mutation frequencies of mutant cells using DSBs with different 4 nt 5' overhangs. (A) Mutation frequencies using NcoI-pRS315URA3. (B) Mutation frequencies using AflII-pRS315URA3.

There are no known unique 4 nt 3' overhang-producing restriction enzymes that were able to cut within either the *LEU2* or *URA3* gene in pRS315URA3. The plasmid pLKL67Y had to be used to create linear form DNA containing a 4 nt 3' overhang using BmtI (Figure 16A). BmtI disrupted the *HIS3* gene in pLKL67Y. The Ura⁺ colonies

grown after transformation were therefore patched and replica plated onto Glu-His plates to measure accuracy. Cells that grew on both Glu-Ura and Glu-His plates were accurately repaired, meaning they were Ura⁺ His⁺, while cells that only grew on Glu-Ura plates were Ura⁺ His⁻ and had inaccurate repair. Just like there was a difference in repair efficiencies, there were also striking differences in repair accuracy between DSBs with 3' overhangs and DSBs with 5' overhangs. Mutants defective for all three complexes had higher error rates when 3' overhangs were present. Mutation frequencies for *mre11*, *dnl4*, and *yku70* cells were 39%, 67%, and 81%, respectively. The numbers for *dnl4* and *yku70* were similar to when 5' overhangs were present (Figure 18 and Figure 20), but mutation frequencies for *mre11* cells were strikingly different (39% for 3' overhangs vs 0% for 5' overhangs) It is not exactly known why this occurs, but the presence or absence of structure-dependent DSB end resectioning could be a contributing factor.

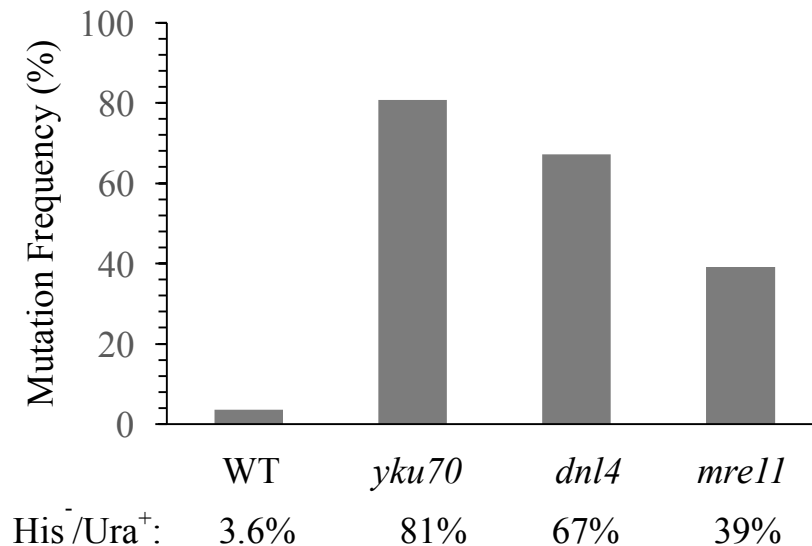


Figure 21. Mutation frequencies of early stationary phase cells using BmtI-cut pRS315URA3. Mutation frequencies were measured using the plasmid BmtI-pLKL67Y.

The final objective of this research was to measure NHEJ repair efficiencies in cell cultures with different levels of G₁. This was done by assessing repair in early stationary, true stationary, and mid-log phase cell cultures. For early stationary phase cells, yeast cells were shaken for ~24 h in YPDA broth at 30°C, while true stationary phase cells were grown on a YPDA plate for 4 days at 30°C. Mid-log phase cells, on the other hand, were grown for 6 h in YPDA broth at 30°C. Each of these cultures were then diluted, sonicated and cell cycle phase distributions were measured. Unbudded cells were recorded as G₁ phase cells, small-budded cells were S phase cells, and large-budded cells were G₂/M cells. Figure 22B depicts the shapes of G₁ phase (unbudded), S phase (small-budded), and G₂/M (large-budded cells). Mid-log phase cells typically contain ~30 to 40% G₁ cells, early stationary phase cultures ~50 to 70% G₁ cells, while true stationary phase cultures contain a G₁ percentage that is typically $\geq 90\%$. These different levels of G₁ cells could potentially have an effect on NHEJ repair efficiency. Figure 22A shows the repair efficiencies of a DSB with 4 nt 5' overhangs (NcoI-pRS315URA3) after transformation using early stationary phase (overnight) cells. These cells were incubated for approximately 24 h in YPDA broth in order to obtain early stationary phase cells. In accordance with the previous results, both the Yku and DNA ligase IV complex mutants had a strong reduction in repair efficiency (120-131 fold), but not the Mrx complex (2 fold). Figure 22C provides evidence that the cells used for this experiment had G₁ percentages ranging from 50-69%.

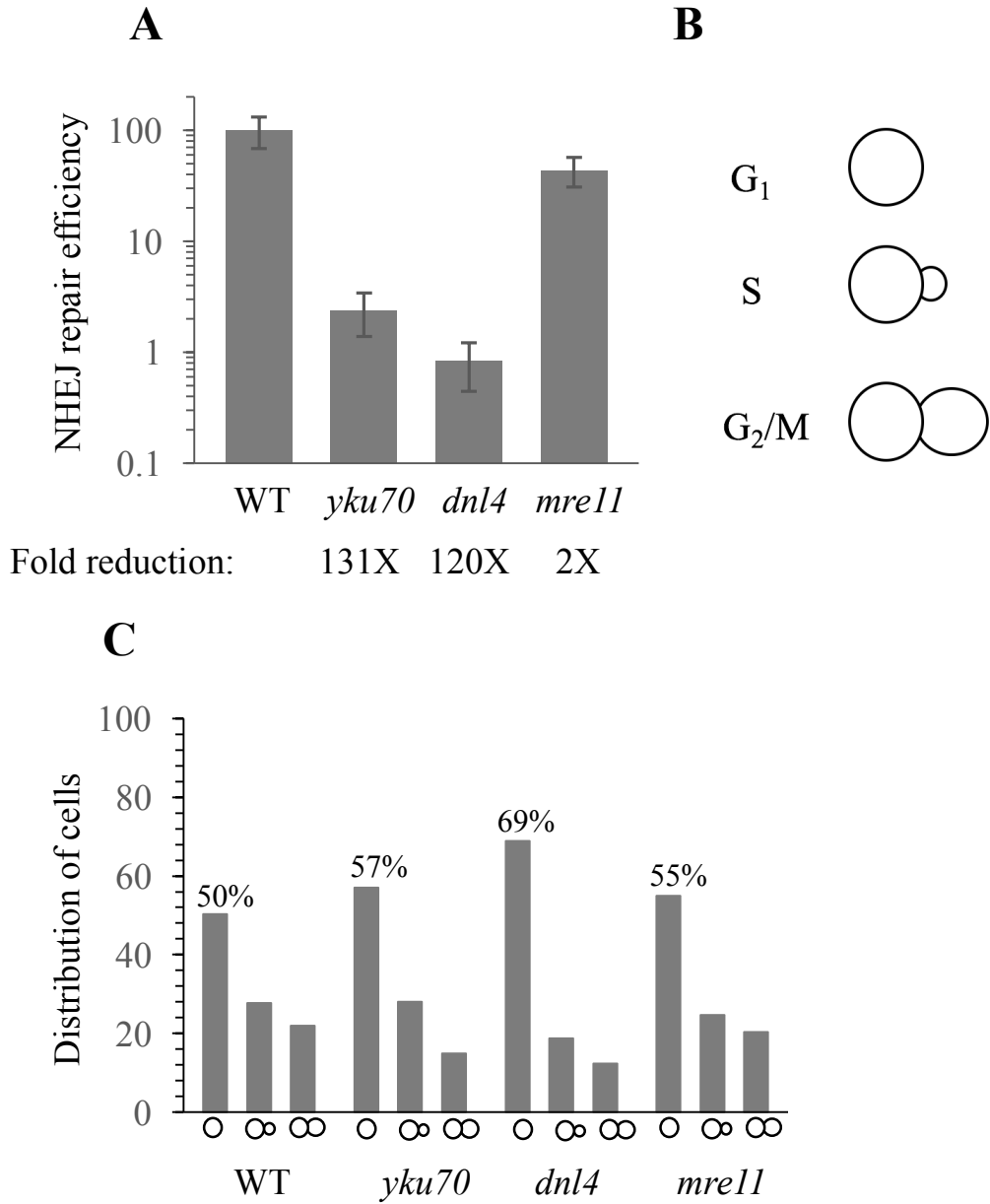


Figure 22. Plasmid repair efficiencies of early stationary phase cells and G₁ percentages within each cell culture. (A) The NHEJ repair efficiencies of mutants in all three complexes were tested. (B) Key showing structural differences in G₁, S, and G₂/M phases of *S. cerevisiae* cells detected using phase contrast microscopy. (C) G₁ (unbudded) percentages in the early stationary phase yeast cell cultures ranged from 50-69%.

To perform NHEJ assays in true stationary phase cells, yeast cells were taken straight from a YPDA plate that had been incubated at 30°C for four days and transformed. Cells in true stationary phase are expected to have a higher percentage of G₁ cells. Figure 23A shows that the Ku complex and DNA ligase IV complex mutants had a strong reduction in repair efficiencies ranging from 48.6 fold to 65.9 fold, while the Mrx complex mutant had only a 2.1 fold reduction. Thus, the stationary phase cultures gave similar results to the early stationary phase cultures. The G₁ percentages measured for the true stationary phase cultures ranged from 81% (*mre11*) to 97% (*yku70*) (Figure 23B). The high percentages of G₁ cells suggest true stationary phase was achieved for this transformation.

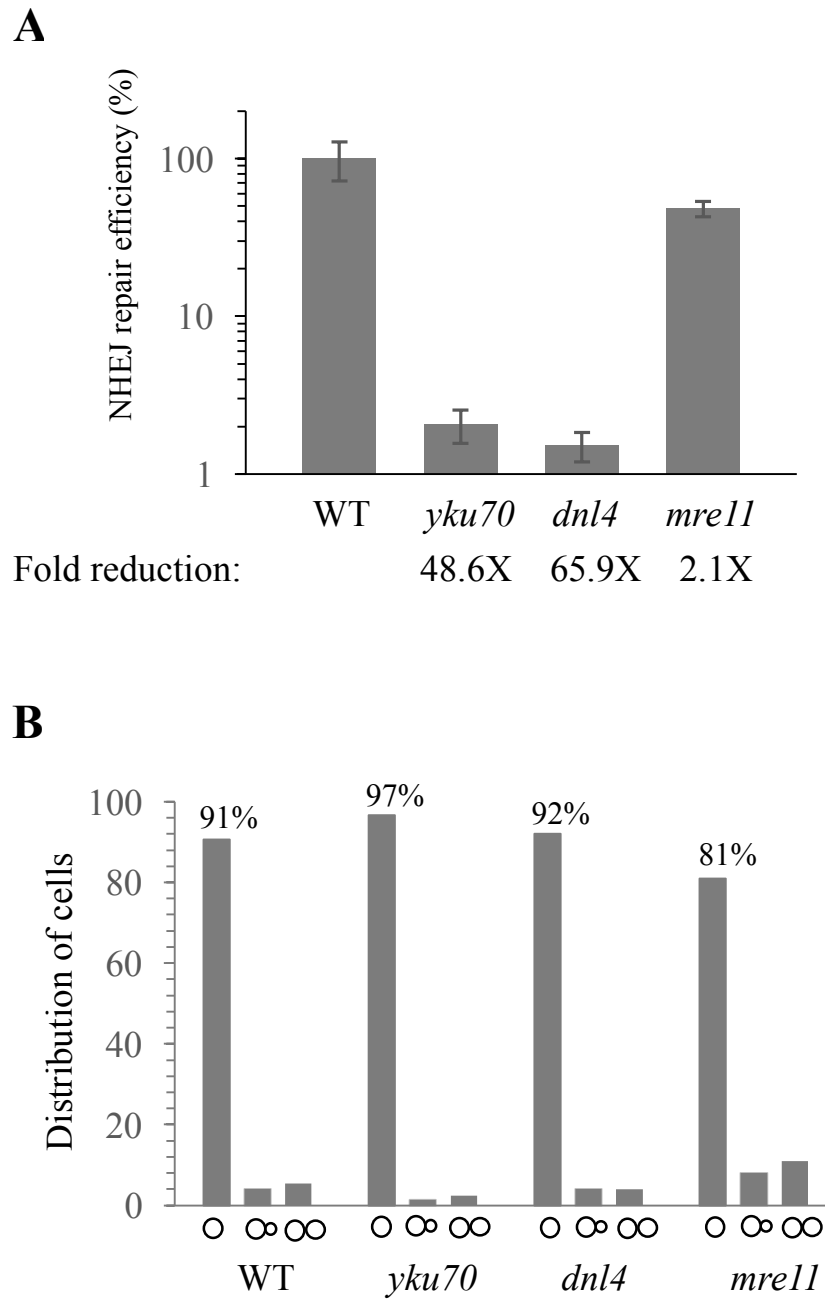


Figure 23. Plasmid repair efficiencies of true stationary phase cells and G_1 percentages. (A) The NHEJ repair efficiencies of mutants in all three complexes during true stationary phase were measured. (B) Percentages of unbudded, small-budded, and large-budded cells in true stationary phase cultures were analyzed.

Yeast cells shaken for 6 h in YPDA broth were used for mid-log phase transformation experiments to measure NHEJ repair efficiencies. These cells were expected to have a lower proportion of G₁ phase cells compared to early and true stationary phase cells, typically only about 30%. It was hypothesized that NHEJ in mid-log phase cells (predominantly S and G₂ phase cells) might exhibit a different dependence on Mrx than cells that are predominantly in G₁. Figure 24B shows that the level of G₁ cells ranged from 16% to 32%. Figure 24A shows evidence supporting this hypothesis. The reductions in repair efficiency in each individual complex mutant were similar. Yku complex mutants had a 3.1 fold reduction, Dnl4 complex mutants had a 3 fold reduction, and Mrx complex mutants had a 4.9 fold reduction (Figure 24A).

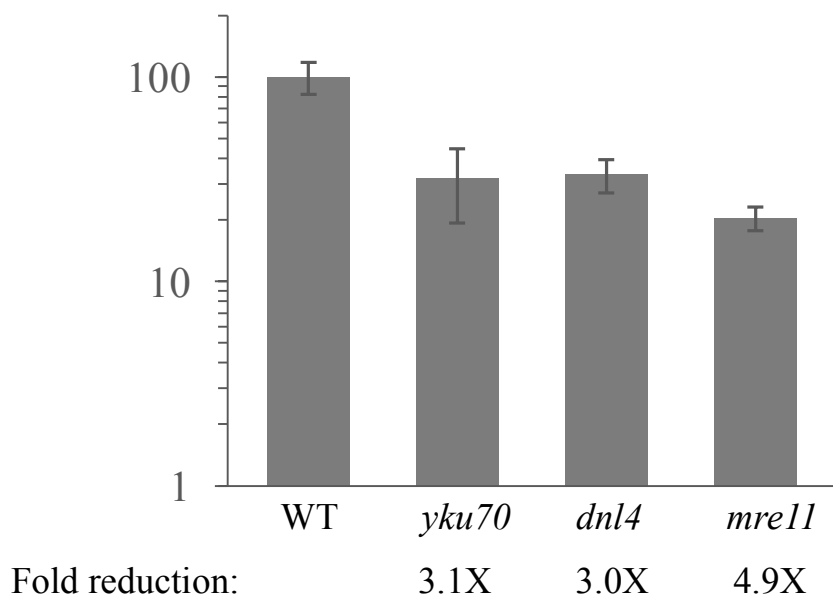
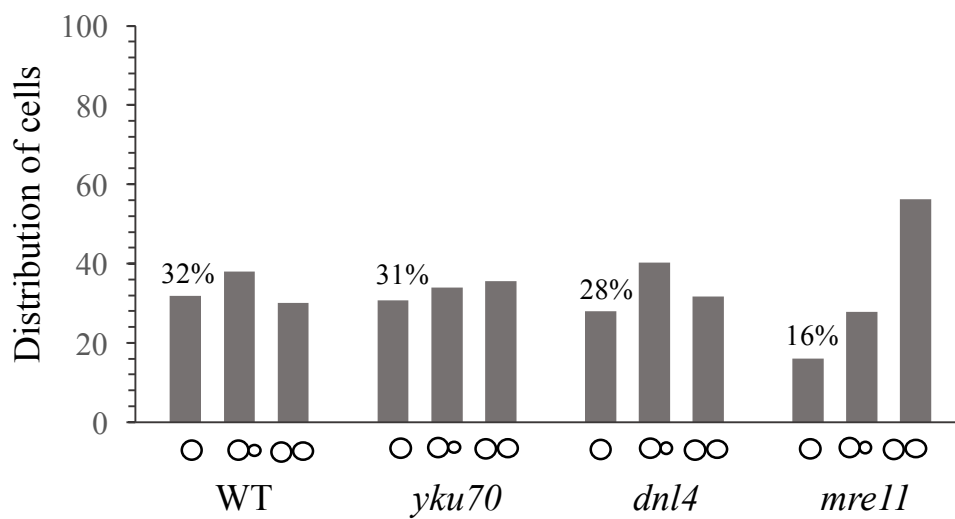
A**B**

Figure 24. NHEJ repair efficiencies of mid-log phase cells using *NcoI*-cut pRS315URA3. (A) The NHEJ repair efficiencies of mutants in all three complexes during mid-log phase were measured. (B) Percentages of unbudded, small-budded, and large-budded cells in mid-log phase cultures were analyzed.

CHAPTER IV

SUMMARY AND CONCLUSIONS

The NHEJ pathway is composed of three protein complexes, the Yku, Mrx, and Dnl4 complexes, which are encoded by eight genes: *YKU70*, *YKU80*, *MRE11*, *RAD50*, *XRS2*, *DNL4*, *LIF1*, and *NEJ1*. Past work has suggested that each complex plays an important role in NHEJ repair. These previous studies (summarized in reference 28) have only tested up to three mutant genes at a time and no previous study analyzed genes encoding all three complexes. In this study, the NHEJ efficiency and accuracy of repair was tested using plasmid assays and all eight genes of the NHEJ pathway. Additional tests analyzed DSBs varying in their structures (5' vs 3' DNA overhangs). The importance of G₁ phase cell numbers in the cell cultures was also examined.

NHEJ repair efficiencies of NcoI-cut pRS315URA3 containing 4 nt 5' overhangs were similar to the results with AflIII-cut pRS315URA3, which also contained 4 nt 5' overhangs but with a different sequence. Repair of both DSBs was strongly decreased in Yku mutants (*yku70* and *yku80*) and DNA Ligase IV mutants (*dnl4*, *lif1* and *nej1*) but not Mrx (*mre11*, *rad50* and *xrs2*) mutants. This result implies that the role of the Mrx complex is much less important than the Yku and DNA Ligase IV complexes in NHEJ repair of DSBs with 5' overhangs. These results also suggest that repair efficiencies with plasmids containing 5' overhangs are sequence independent.

The same NHEJ repair assays were performed using repair of BmtI-cut pLKL67Y DNA, which contained 3' overhangs. In contrast to the DNAs with 5' overhangs, BmtI-cut pLKL67Y showed a similar reduction in repair efficiency in mutants of all three

complexes. This gives evidence that the Mrx complex has a more important role in NHEJ repair of DSBs that contain 3' overhangs. Results with different DSB structures are summarized in Figure 25. It is not clear why plasmids with 3' ssDNA overhangs do not get repaired in *mre11* mutants even though these cells are Yku⁺ and DNA Ligase IV⁺. One possibility is that, in the absence of Mrx, DSB ends with 3' tails are acted on by nucleases and the degraded DNAs are never able to complete repair by NHEJ. Liang et al. (2016) presented evidence that the physical association of Mrx with Yku70/80 stabilizes chromosomal DSB end with 3' overhangs more than DSB with 5' overhangs (46). If this is true, strong candidates for this degradation are Exo1 and Sgs1-Dna2. These nucleases normally act on DNA substrates in the HR pathway that have long 3' ssDNA tails and they may also have affinity for the 3' overhangs produced by BmtI, though these tails are very short (Figure 26) (39).

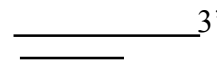
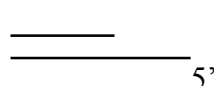
BmtI		NcoI or AflIII	
			
	NHEJ		NHEJ
<u>Mutant</u>	<u>repair</u>	<u>Mutant</u>	<u>repair</u>
<i>yku70</i>	---	<i>yku70</i>	---
<i>dnl4</i>	---	<i>dnl4</i>	---
<i>mre11</i>	---	<i>mre11</i>	~+

Figure 25. Repair efficiencies determined using DSB with 3' and 5' DNA overhangs. All mutants (*yku70*, *dnl4*, and *mre11*) were strongly deficient in NHEJ repair except for *mre11* cells when 5' DNA overhangs were present.

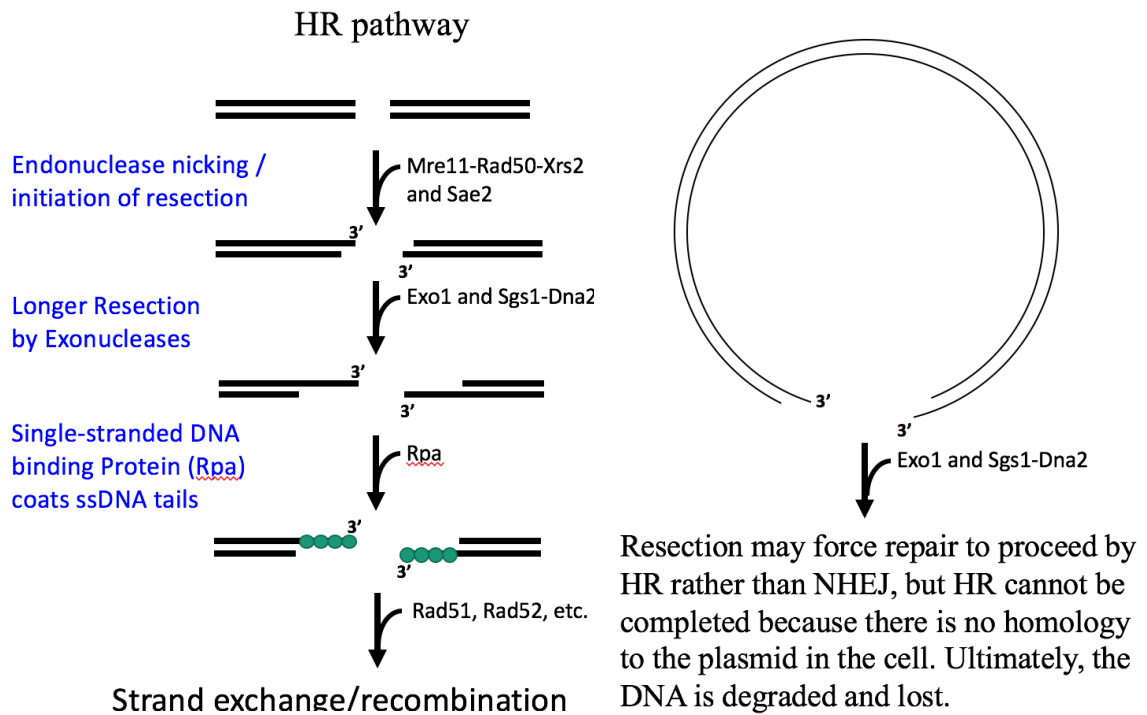


Figure 26. Similarities between the HR pathway and plasmid with 3' overhangs. The similarities between the second step of the HR pathway and a plasmid with 3' overhangs may cause large amounts of resectioning by Exo1 and Sgs1-Dna2.

The NHEJ repair accuracies observed using NcoI- and AflIII-cut pRS315URA3 DNA containing 5' overhangs were similar to each other. Mutation frequencies were high in *yku70* and *dnl4* mutants, but near WT in *mre11* cells. As for repair accuracies on plasmids with 3' overhangs, the mutation frequency of *mre11* cells was much higher than WT, near those of *dnl4* and *yku70* cells. The rejoining of these DSB ends in *dnl4* and *yku70* and *mre11* mutants cannot occur by conventional NHEJ and also cannot be performed by the HR pathway (there is no homology). This means that colonies forming in e.g., *dnl4* mutants are due to repair by another method, likely ultimately involving

ligation of the ends by the major DNA ligase in yeast cells, called Cdc9. It is not clear yet how this NHEJ- and HR-independent repair process leads to high levels of mutations in the recircularized plasmids.

Another objective of this project was to measure the differences in NHEJ repair efficiency in cell cultures having different levels of G₁ phase cells (early stationary, true stationary, and mid-log). Early stationary phase cell cultures (50-69% G₁ cells) and true stationary phase cells (~90% G₁) showed a strong reduction in NHEJ efficiency in *yku70* and *dnl4* mutants but not in *mre11* mutants (Figure 22 and Figure 23). When cell cultures were grown to mid-log phase, which contained G₁ levels of about ~20% to 30%, NHEJ repair efficiencies were decreased to similar levels in the three mutants (Figure 24). It is known that the NHEJ pathway is most active during G₁ phase (32, 42, 45, 49). This is logical due to G₁ cells not having any sister chromatids to use for repair by homologous recombination (HR). It is known that there is inhibition of resectioning during G₁ which promotes NHEJ as the preferred repair pathway of choice during this phase. The experiments performed here found that DSBs with 5' overhangs did not require Mre11 when the cells were mostly G₁ (early and true stationary phase cells), but MRE11 was as important as *YKU70* and *DNL4* when only ~20-30% of the cells were in G₁, i.e., when the cells were mostly in S and G₂ phases. These results suggest that the NHEJ pathway is not only more active in G₁, but may also have different requirements for the Mrx complex in G₁ versus S and G₂.

As shown in Table 2, five research papers have been published previously that analyzed plasmid DSB repair in mutants defective in at least two of the three major

NHEJ complexes. All yeast cells tested in these papers were in mid-log phase and contained similar of reductions in NHEJ

repair efficiencies (10X-40X) among all mutants (*yku70*, *yku80*, *dnl4*, *nej1*, and *rad50*). The similar requirements for each complex in repair efficiency is in agreement with the mid-log phase cell results observed in this project.

Table 2. Five other studies involving NHEJ repair assays on mid-log phase cells. Previous studies involving NHEJ repair of plasmid DNA used mid-log phase cells. The repair efficiencies were similarly reduced regardless of complex.

PAPER	REF.#	TRANSFORMED CELLS	ENZYME	OVERHANGS	<i>yku70</i>	<i>yku80</i>	<i>dnl4</i>	<i>nej1</i>	<i>rad50</i>
MILNE <i>et al.</i>	47	Log Phase	BamHI	5' (4nt)	14X	10X			12X
VALENCIA <i>et al.</i>	48	Log Phase	BamHI	5' (4nt)	20X			40X	
KARATHANASIS AND WILSON	49	Log Phase	KpnI	3' (4nt)	18X		18X		
LEWIS <i>et al.</i>	50	Log Phase	NcoI	5' (4nt)	19X				15X
BAHMED <i>et al.</i>	51	Log Phase	HindIII	5' (4nt)		11X	30X		

REFERENCES

1. Helleday, T., Eshtad, S., and Nik-Zainal, S. An Overview of types of DNA damage and casual agents. *Nature*. (2014) *Nature* **15**, 585-598
2. Ward, J.F., DNA damage produced by Ionizing Radiation In mammalian cells: identities, mechanisms of formation, and reparability (1988) *Nucleic Acid Res.* **35**, 95-125
3. Kato, H., Induction of sister chromatid exchanges by chemical mutagens and its possible relevance to DNA repair (1974) *Exp. Cell Res.* **85**, 239-247
4. Setlow, R.B., DNA Repair Pathways (1980) *Basic Life Sci.* **15**, 45-54
5. Ohnishi, T., Mori, E., and Takahashi, A. DNA double-stranded breaks: Their production, recognition and repair in eukaryotes (2009) *Mutat. Res.* **669**, 8-12
6. Hefferin, M.L., and Tomkinson, A.E. Mechanism of DNA double-stranded break repair by non-homologous end joining. *DNA Repair* (2005) **4**, 639-648
7. Burma, S., Chen, B.P.C., and Chen, D.J. et al. Role of non-homologous end joining (NHEJ) in maintaining genomic integrity, (2006) *DNA Repair* **5**, 1042-1048
8. Lewis, L.K., and Resnick, M.A. Tying up loose ends: nonhomologous end-joining in *Saccharomyces cerevisiae* (2000) *Mutat. Res.* **451**, 71-89
9. Wyman, C., and Kanaar, R. DNA double-stranded break repair: all's well that ends well (2006) *Annu. Rev. Genet.* **40**, 363-383

10. Critchlow, S.E., and Jackson, S.P. DNA end-joining: from yeast to man (1998) *Cell* **10**, 394-398
11. Essers, J., Houtsmuller, A., Veelen, L.V., Paulusma, C., Nigg, A.L., et al Nuclear dynamics of RAD52 group homologous recombination proteins in response to DNA damage (2002) *EMBOJ* **8**, 1881-2053
12. Fell, V.L., and Schild-Poulter, C. The Ku heterodimer: Function in DNA repair and beyond (2015) *Mutat. Res. Rev. Mut. Res.* **763**, 15-29
13. Nemazee, D. Mechanisms of Central tolerance for B cells (2017) *Nature*. **17**, 281-294
14. Schatz, D.G. V(D)J Recombination (2002) *Mutat. Res.* **200**, 5-11
15. Boubnov, N.V., and Weaver, D.T, *scid* Cells are Deficient in Ku and Replication Protein A Phosphorylation by the DNA-Dependant Protein Kinase (1995) *Mol. and Cell Bio.* **10**, 5700-5706
16. Porter, S.E., Greenwell, P.W., Ritchi, D.B., and Petes, T.D. The DNA-binding protein HDF1p (a putative Ku homologue) is required for maintaining normal telomere length in *Saccharomyces cerevisiae* (1996) *Nucleic Acids Res.* **24**, 582-585
17. Bouton, S.J., and Jackson, S.P. Identification of a *Saccharomyces cerevisia* Ku 80 homologue: roles in DNA double strand break rejoining and in telomeric maintenance (1996) *Nucleic Acids Res.* **24**, 4639-4648
18. Gravel, S., Larrivee, M., Labrecque, P., and Wellinger, R.J. Yeast Ku as a regulator of chromosomal DNA end structure (1998) *Science* **280**, 741-744

19. Holland, C.L., Wasko, B.M. Sanderson, B.A., Titus, J.K., Riojas, A.M., and Lewis, L.K. Suppression of telomere instability in *Saccharomyces cerevisiae yku70* mutants by Est2 polymerase in DNA repair and reverse transcriptase-independent (2017) Submitted to Current Genetics **1**, 3-6
20. Krogh, B.O., and Symington, L.S. Recombination proteins in yeast (2004) Annu. Rev. Genet. **38**, 322-271
21. Stewart, G.S., Maser, R.S., Stankovic, T., Bressari, D.A, Kaplan, M.I., *et al.* The DNA double-stranded break repair Gene hMRE11 is mutated in individuals with an Ataxi-Telangiectasia-like Disorder (1999) Cell **99**, 577-587
22. Anderson, D.E., Trujillo, K.M., and Erickson, H.P. Structure of Rad50 and Mre11 DNA repair complex from *Saccharomyces cerevisiae* by electron microscopy (2001) J. Biol. Chem. **276**, 37027-37033
23. Wiltzuis, J.J., Hohl, M., Fleming, J.C., and Petrini, J.H. The Rad50 hook domain is a critical determinant of Mre11 complex functions (2005) Nat. Struct. Mol. Biol. **12**, 403-407
24. Trujillo, K.M., Roh, D.H., Chen, L., Komen, V., Tomkinson, A., and Sung, P. Yeast Xrs2 binds DNA and helps target Rad50 and Mre11 to DNA ends (2003) J. Biol. Chem. **278**, 48957-48964
25. Simone, J.Z., Petersen, S., Tessarollo, L., Nussenzweig, A., *et al.* Targeted disruption of the Nijmegen breakage syndrome gene NBS1 leads to early embryonic lethality in mice (2001) Curr. Biol. **11**, 105-109

26. Dore, A.S., Furnham, N., Davies, O.R., Sibanda, B.L., Chirgadze, D.Y., *et al.*
Structure of an Xrcc4-DNA ligase IV yeast ortholog complex reveals a novel
BRCT interaction mode (2006) *DNA Repair* **5**, 362-368
27. Valencia, M., Bentele, M., Vaze, M.B., Herrmann, G., *et al.* NEJ1 controls non-
homologous end-joining in *Saccharomyces cerevisiae* (2001) *Nature* **414**, 666-
669
28. Lilly, J.L., Analysis of NHEJ DNA repair efficiency and accuracy in new mutants
of *Saccharomyces cerevisiae* (2015) Master's thesis, Texas State University
29. Tripp, J.D., Lilley, J.L., Wood, W.N., and Lewis, L.K. Enhancement of plasmid
DNA transformation efficiencies in early stationary phase yeast cell cultures
(2013) *Yeast* **30**, 191-200
30. Gietz, R.G., and Woods, R.A., Yeast transformation by the LiAc/SS carrier
DNA/PEG method. *Methods in Molec. Biol.: Yeast Protocols* **2**, 107-120
31. Chen, X., and Tomkinson, A.E. Yeast Nej1 is key participant in the initial end
binding and final ligation step of nonhomologous end-joining (2011) *J. Biol.*
Chem. **286**, 4931-4932
32. Gao, S., Honey, S., Futcher, B., and Grollman, A.P. The nonhomologous end-
joining pathway of *S. cerevisiae* works effectively in G₁-phase cells, and relegates
cognate ends correctly and non-randomly (2016) *DNA Repair*. **42**, 1-10
33. Lieber, M.R., The mechanism of double-strand DNA break repair by the
nonhomologous DNA end-joining pathway (2010) *Annu. Rev. Biochem.* **79**, 181-
211

34. Roberts S. A., Strande, N., Burkhalter M. D., Strom C., Havener J. M., Hasty P., Ramsdend D. A. (2010) Ku is a 5'-dPR/AP lyase that excises nucleotide damage near broken ends. *Nature* **464**, 1214-1217
35. Strande N., Roberts S. A., Oh, S., Hendrickson, E.A., Ramsden D.A., (2012) Specificity of the dRP-AP lyase of Ku promotes nonhomologous end-joining (NHEJ) fidelity at damaged ends. *J Biol Chem* **287**, 13686-13693
36. Dudasova Z., Dudas A., Chavanec M. (2004) Non-homologous end-joining factors of *Saccharomyces cerevisiae*. *FEMS Microbiol Rev* **28**, 581-601
37. Rathaus M., Lerrer B., cohen H.Y. (2009) Deubiquitylation: a novel DUB enzymatic activity for the DNA repair protein, Ku70. *Cell Cycle* **8**, 1843-1852
38. Lieber M. R., (2010) The mechanism of double-strand DNA break repair by the non-homologous DNA end-joining pathway. *Annu. Rev. Biochem* **79**, 181-211
39. Gobbin, E., Cassani, C., Villa, M., Bonettie, D., and Longhese, M. P. Functions and regulation of the MRX complex at DNA double-strand breaks (2016) *Microb Cell*. **3**, 329-331
40. Liao, S., Tamaro, M., and Yan, H. The structure of ends determines the pathway choice and Mre11 nuclease dependency of DNA double-strand break repair (2016) *Nucleic Acids Res.* **12**, 5689-5701
41. Daley, J.M., Palmbo, P.L., and Wu, Dongliang, *et al.* Nonhomologous end-joining in yeast (2005) *Annu. Review of Genetics.* **39**, 431-451
42. Emerson, C.H., and Bertuch, A.A. Consider the Workhorse: Nonhomologous end-joining in budding yeast. (2016) *Biochem. Cell Biol.* **94**

43. Bahmed, K., Karin, A.S., Nitiss, C., and Nitiss, J.L. End-processing during non-homologous end-joining: a role for exonuclease 1 (2011) *Nucleic Acids Res.* **39**, 970-978
44. Lewis, L.K., Karthikeyan, G., Cassiano, J., and Resnick, M.A. Reduction of nucleosome assembly during new DNA synthesis impairs both major pathways of double-strand break repair. (2005) *Nucleic Acids Res.* **33**, 4928-4939
45. Karathanasis, E., and Wilson, T.E. Enhancement of *Saccharomyces cerevisiae* end-joining efficiency by Cell growth stage but not by impairment of recombination. (2002) *Genetics* **161**, 1015-1027
46. Liang, Z., Sunder, S., Nallasivam, S., and Wilson, T.E. Overhang polarity of chromosomal double-strand breaks impacts kinetics and fidelity of yeast non-homologous end joining. (2016) *Nucleic Acid. Res.* **44**, 2769-2781
47. Milne, G.T., Jin, S., Shannon, K.B., and Weaver, D.T., Mutations in two ku homologs define a DNA end-joining repair pathway in *Saccharomyces cerevisiae* (1996) *Mol. And Cell. Bio.* **16**, 4189-4198
48. Valencia, M., Bentele, M., Vaze, M.B., et al. NEJ1 controls non-honologous end joining in *Saccharomyces cerevisiae* (2001) *Nature.* **414**, 666-669
49. Karathanasis, E., and Wilson, T.E., Enhancement of *Saccharomyces cerevisiae* end-joining efficiency by cell growth stage but not by impairment of recombination. (2002) *Genetics.* **161**, 1015-1027
50. Lewis, L.K., Karthikeyan, G., Cassiano, J., and Resnick, M.A. Redcution of nucleosome assembly during new DNA synthesis impairs both major pathways of double-strand break repair. (2005) *Nucleic Acid. Res.* **33**, 4928-4939

51. Bahmed, K., Nitiss, K.C., and Nitiss, J.L. Yeast Tdp1 regulates the fidelity of nonhomologous end-joining. (2010) PNAS Proc. Natl. Acad. Sci. USA **107**, 4057-4062